INTERNATIONAL JOURNAL FOR NUMERICAL AND ANALYTICAL METHODS IN GEOMECHANICS
Int. J. Numer. Anal. Meth. Geomech., 2007; **31**:607–648
Published online 26 September 2006 in Wiley InterScience (www.interscience.wiley.com). DOI: 10.1002/nag.552

Natural vibration characteristics of gravity structures‡

Ashok K. Chugh*,†

U.S. Bureau of Reclamation, P.O. Box 25007, Denver, CO 80225, U.S.A.

SUMMARY

A forced vibration procedure is presented to estimate fundamental and higher frequencies of vibrations and associated mode shapes of gravity structures. The gravity structures considered are retaining walls and gravity dams. The validity of the proposed procedure is tested on three test problems of varying complexity for which the natural vibration frequencies and mode shapes either have known analytical solutions or have been determined via numerical means/field tests by others. Also included are the results of natural vibration frequencies and associated mode shapes for a spillway control structure located near the abutment end of an embankment dam obtained using the proposed procedure. For all problems considered, fundamental frequency and mode shape results using the proposed procedure are compared with the results obtained using an alternative procedure in which static deflections due to the structure's own weight are used as the starting point for free vibrations by setting the gravity vector to zero. All results compare well. The merits of the proposed procedure are discussed. Published in 2006 by John Wiley & Sons, Ltd.

Received 30 March 2006; Revised 10 July 2006; Accepted 11 July 2006

KEY WORDS: vibration; frequency; mode shape; natural; sinusoid; excitation; retaining wall; spillway; dam

1. INTRODUCTION

All natural and constructed systems vibrate at varying frequencies and have associated mode (deformed) shapes, and these vibration characteristics are unique for every system. Also, all vibrating systems respond to an external vibrating stimulus to varying extents. Damping is another unique characteristic of every vibrating system and affects the vibrating system's response to external stimulus. Determination of frequencies of vibrations, associated mode shapes, and damping of a system is a prerequisite in studying time-dependent behaviour of the system subjected to an external vibrating stimulus; it is equally important to know the characteristics of the vibrating stimulus.

*Correspondence to: Ashok K. Chugh, U.S. Bureau of Reclamation, P.O. Box 25007, Denver, CO 80225, U.S.A.
†E-mail: Achugh@do.usbr.gov

Published in 2006 by John Wiley & Sons, Ltd.

Numerical and analytical procedures have been developed to perform static and dynamic analyses of systems/structures. Analytical aspects of structural dynamics involve complex mathematical formulations; numerical analysis procedures implemented in computer programs offer some relief from the mundane tasks of problem solving. For simple problems, results from numerical model studies are compared with those obtained using analytical procedures. For complex systems such as dams and reservoirs, multi-storey buildings, and other constructed facilities, numerical procedures are used exclusively to determine likely response of the system to a dynamic event. Sometimes, field tests are performed to determine natural frequencies, mode shapes, and damping by actually shaking full-scale structures using vibration generators or explosives and measuring responses of the structure at several locations. Results of these field tests provide insights into the complexities of dynamic interactions of the system(s) tested, which, in turn, result in development of improved and validated numerical analysis procedures.

The objectives of this paper are to present:

(a) a simple, effective, and efficient numerical procedure for calculating natural frequencies of vibrations and associated mode shapes for gravity structures;
(b) results of natural vibration characteristics for three test problems of varying complexity using the proposed procedure; and
(c) results of natural vibration characteristics for a concrete spillway control structure located near the abutment end of an embankment dam using the proposed procedure.

For objective (a), analytical aspects of the proposed procedure are included and results checked via numerical means. For objective (b), results from numerical analyses of the test problems using the proposed procedure are compared with those reported by others. For objective (c), results from the numerical analyses using the proposed procedure are compared with those obtained using an alternative procedure in which static deflections due to structure's own weight are used as the starting point for free vibrations by setting the gravity vector to zero [1]. Also, results from the use of the alternative procedure for all problems considered are included in Appendix A. All structural materials are assumed to be homogeneous, isotropic, and linearly elastic; and only small amplitude vibrations without damping are considered.

The proposed procedure can be implemented in essentially any continuum-mechanics-based dynamic analysis program. For the test and sample problems presented in this paper, commercially available computer programs FLAC [2] and FLAC3D [3] were used. FLAC and FLAC3D are acronyms for Fast Lagrangian Analysis of Continua in two- and three-dimensions, respectively; they are explicit finite difference programs, and their adoption was for convenience.

It is interesting and also considered instructive to view the development of mode shapes of a structure—especially the ones associated with higher frequencies—in case it becomes desirable to suppress/alter (by external means) some of the modes from developing during a dynamic event. For this purpose, displays of the deformed configurations (mode-shapes) during the dynamic analyses of the problems included in this paper were captured in the form of movies. Copies of these movie displays can be obtained from the author on request. Software necessary to run these movie displays is also included.

Terminology and symbols used in this paper are typical of those used in structural dynamics texts. For frequency, the two commonly used descriptors f (cycles/s or Hz) and ω (rad/s) are used either interchangeably or both appear together. Also, a pulse is usually described by

Published in 2006 by John Wiley & Sons, Ltd. *Int. J. Numer. Anal. Meth. Geomech.* 2007; **31**:607–648
DOI: 10.1002/nag

amplitude and duration (period) in preference to amplitude and frequency; however, in this paper, these descriptors are used interchangeably. Three-dimensional (3-D) geometry is in x, y, z co-ordinate system with z-axis being vertical and x–z plane being the plane of the paper. The x, y, z co-ordinate system follows the right-hand rule. Two-dimensional (2-D) geometry is in the x–z plane; u, v, w refer to displacements in the x, y, z co-ordinate directions, respectively. Transverse refers to the x-direction; vertical refers to the z-direction; and longitudinal refers to the y-direction. References to textbooks included in the paper are representative but not a complete list on the subject.

2. RATIONALE FOR THE PROPOSED PROCEDURE

The proposed procedure is for determination of all natural frequencies ($\omega_n = 2\pi f_n$ for $n = 1, 2, 3, \ldots$) of vibrations and the associated natural mode shapes (ψ_n for $n = 1, 2, 3, \ldots$) of gravity structures, and has two primary steps: step (a) is for calculating natural frequencies of vibrations, and step (b) is for calculating natural mode shapes.

Step (a) involves only one dynamic analysis of the structural system for all (N) natural frequencies of the structural system; and step (b) involves N dynamic analyses for all N natural mode shapes of the structural system—one for each of the natural frequencies determined in step (a).

In both steps (a) and (b), the excitation function is a force function $f(t)$. In step (a) analysis, the force function is a sine pulse of one complete cycle (non-periodic) followed by zero force for the duration of dynamic analysis; in step (b) analysis, the force function is a continuous train of sine pulses (periodic) of prescribed frequency for the duration of the dynamic analysis.

In broad terms, the proposed procedure follows the general principles involved in forced vibration tests to measure natural vibration characteristics of full-scale structures in the field [4, 5]. A brief description of the field test using mechanical vibrators to determine natural vibration characteristics of a concrete gravity dam is included in Section 6, test problem 3. Rationale for the development of the proposed procedure for determining natural frequencies and associated mode shapes are described below separately.

2.1. Natural frequencies of vibrations

A full-cycle sine pulse (force–time integral = 0) has in it a wide range (band) of frequencies ω_a ($= 2\pi f_a$); see Section 3 for analytical and numerical details. Therefore, a structure subjected to a full-cycle sine pulse excitation will experience large responses whenever one of the frequencies (ω_a or f_a) in the applied excitation approaches one of the structure's natural frequencies of vibration (ω_n or f_n); and with no damping, these extremes in the structure's responses will reverberate (continue) undiminished past the duration of the sine pulse. These spikes in the structure's responses can be identified via a fast Fourier transform (FFT) power spectrum analysis of the response (time-history) data at some identified location(s) on the structure. In general, the excitation function can be a force, ground displacement, ground velocity, or ground acceleration; the structure's response can be displacement, velocity, or acceleration; and the identified response location for time-history can be any grid point on the structure that is not constrained by a prescribed boundary condition and is not a node

Published in 2006 by John Wiley & Sons, Ltd. *Int. J. Numer. Anal. Meth. Geomech.* 2007; **31**:607–648
DOI: 10.1002/nag

(stationary point in a vibration mode shape). Thus, if we make a dynamic analysis of a numerical model of a structure for a full-cycle sine pulse excitation followed by free vibrations for some length of time and record the time history of the structure's response at some location(s), then this response will have all the information on resonances and hence all of the structure's natural frequencies, and an FFT power spectrum analysis of the response data will reveal all of the natural frequencies of the structure. A structure with distributed mass and elasticity (continuum) has an infinite number of degrees-of-freedom (d.o.f.) and hence, an infinite number of natural frequencies. However, a discretized model of the structure has a finite number of d.o.f. and hence, a finite number of natural frequencies. By increasing the number of grid lines dividing the continuum (into smaller zones), the numerical model can be made to approximate the continuum to a desired degree. This explains the motivation in developing the proposed procedure for determining all natural frequencies of a system.

2.2. Natural mode shapes of vibrations

It is well known that if a structure is subjected to a continuous train of sinusoidal excitation of a single frequency (ω_0 or f_0), then the structure's response is oscillatory, and the deformed shape (ψ_0) of the structure corresponds to the frequency of the sinusoidal excitation (ω_0 or f_0). See Section 3 for analytical and numerical details. Therefore, if we make a dynamic analysis of the numerical model (the same as used for natural frequencies determination) of the structure for a periodic sinusoidal excitation of natural frequency (say ω_k or f_k) for some length of time, and at the end of the dynamic analysis, plot the deformed configuration of the model, the plot will be uniquely the kth natural mode shape (ψ_k) corresponding to the kth natural frequency (ω_k or f_k) of the structure. Thus, by repeating the dynamic analysis for each of the natural frequencies and, at the end of each dynamic analysis, plotting the deformed configuration of the model, we get all N natural mode shapes of the structure. This was the motivation in developing the proposed procedure for determination of natural mode shapes.

2.3. Location of excitation force

The location for application of the excitation force can be any grid point on the numerical model that is not constrained by a prescribed boundary condition and is not a nodal point of a natural mode. If an exciting force is applied at the nodal point of a natural mode, that mode will not enter into the response. Also, if an exciting force is applied at a point of maximum displacement for a mode, the mode will show a maximum response.

3. DETAILS OF THE PROPOSED PROCEDURE

The proposed procedure uses forced vibrations to calculate natural vibration characteristics of gravity structures and follows the rationale explained in Section 2. The procedure uses: (a) a non-periodic sinusoidal pulse excitation and resonance criterion to determine natural frequencies; and (b) a periodic sinusoidal excitation of select natural frequency and resonance criterion to determine the associated mode shape.

3.1. Natural frequencies of vibrations

A non-periodic sinusoidal pulse of angular frequency $\omega_0 = 2\pi f_0$ (duration $t_0 = 2\pi/\omega_0$) has in it a wide range of frequencies. Therefore, if a structure in its undeformed configuration is excited by such a pulse force, the structure's response should resonate at (and near) all its natural frequencies that find a match with the frequencies in the excitation pulse. The response parameter selected is displacement. Thus, an FFT power spectrum analysis of the computed displacement–time history data of the structure provides the natural frequencies of the structure. The analytical and numerical details for the frequency spectrum of a full-cycle sinusoidal pulse are described below separately.

3.1.1. Analytical formulation. The frequency spectrum $F(\omega)$ of a non-periodic wave form $f(t)$ is generally obtained using the Fourier transform of the wave form. For a time history $f(t)$ of finite duration $0 \leqslant t \leqslant t_d$, the frequency spectrum $F(\omega)$ is expressed as

$$F(\omega) = \int_{t=0}^{t_d} f(t) \mathrm{e}^{-\mathrm{i}\omega t}\, \mathrm{d}t \tag{1}$$

where $\mathrm{e}^{-\mathrm{i}\omega t} = \cos(\omega t) - \mathrm{i}\sin(\omega t)$.

For a full-cycle sinusoidal pulse of frequency ω_0 and amplitude p_0, Figure 1(a), Equation (1) becomes

$$F(\omega) = p_0 \int_{t=0}^{t_0} \sin(\omega_0 t) \mathrm{e}^{-\mathrm{i}\omega t}\, \mathrm{d}t \tag{2}$$

Evaluation of Equation (2) using $t_0 = 2\pi/\omega_0$ leads to

For $\omega \neq \omega_0$

$$F(\omega) = \mathrm{i}\frac{2p_0\omega_0}{\omega_0^2 - \omega^2} \sin\left(\frac{\omega}{\omega_0}\pi\right) \mathrm{e}^{-\mathrm{i}(\omega/\omega_0)\pi} \tag{3}$$

For $\omega = \omega_0$, Equation (3) is evaluated in the limit as $\omega \to \omega_0$ using L'Hôpital's rule for evaluation of a function taking on an indeterminate form [6]

$$\underset{\omega \to \omega_0}{Lt}\, F(\omega) = -\mathrm{i}\frac{p_0\pi}{\omega} \mathrm{e}^{-\mathrm{i}(\omega/\omega_0)2\pi} \tag{4}$$

From Equations (3) and (4), distribution of absolute value of amplitudes in the frequency spectrum is:

For $\omega \neq \omega_0$

$$|F(\omega)| = \left|\frac{2p_0}{\omega_0} \frac{1}{1 - (\omega^2/\omega_0^2)} \sin\left(\frac{\omega}{\omega_0}\pi\right)\right| \tag{5}$$

and for $\omega = \omega_0$

$$|F(\omega_0)| = \frac{p_0\pi}{\omega_0} \tag{6}$$

In Equations (2)–(6), variables with subscript 0 refer to the sine pulse, and those without a subscript refer to the frequency spectrum.

Figure 1(b) is a plot of Equations (5) and (6) for $p_0 = 1$ N, and $\omega_0 = 2\pi$ rad/s. In this plot, the x-axis represents normalized values of f/f_0 where $f = \omega/(2\pi)$ and $f_0 = \omega_0/(2\pi)$; and the plot is limited to $0 \leqslant f/f_0 \leqslant 10$.

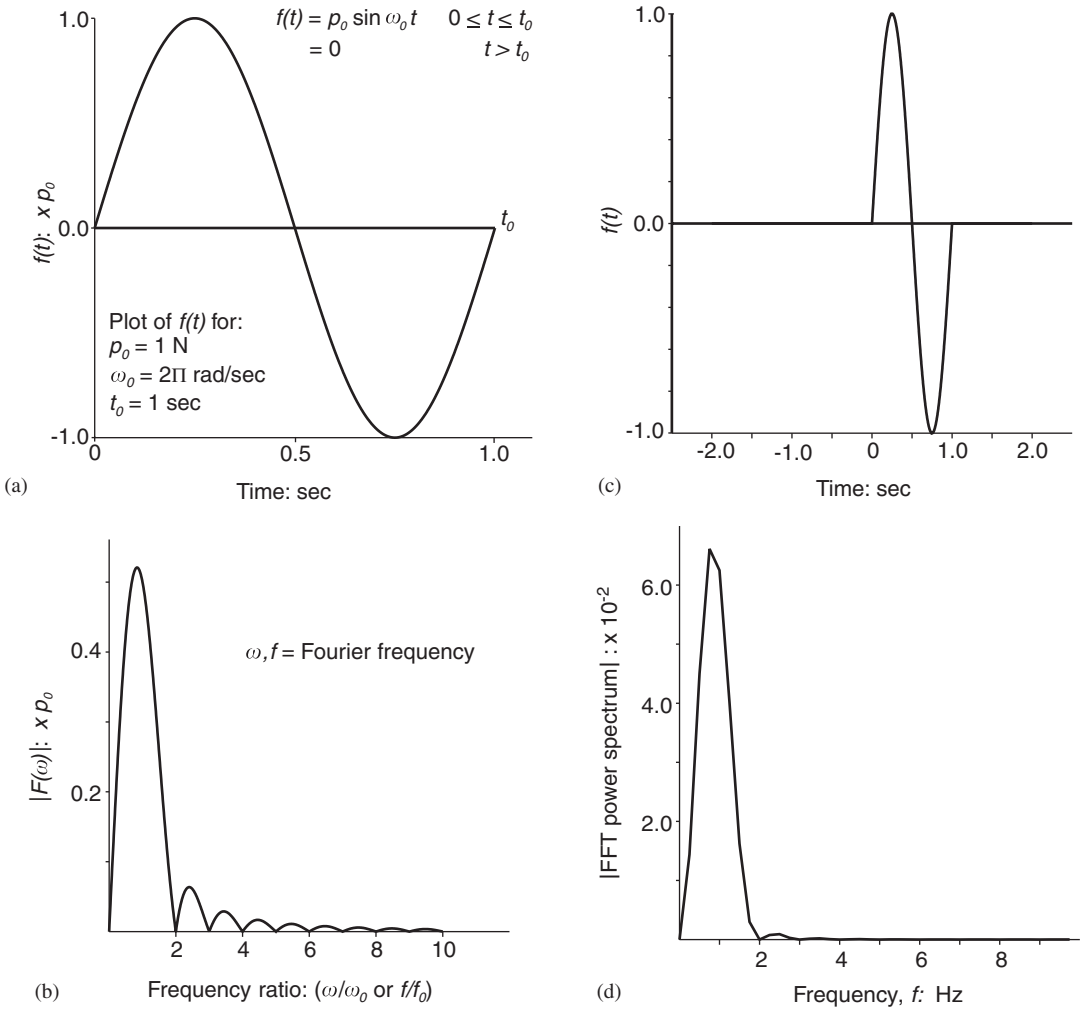

Figure 1. Characteristics of a full-cycle sine pulse: (a) definition; (b) frequency spectrum using Equations (5) and (6); (c) sine pulse (a) with zero padding; and (d) FFT power spectrum of (c).

3.1.2. Numerical verification. The sine pulse of Figure 1(a) for $p_0 = 1$ N, and $\omega_0 = 2\pi$ rad/s was modified by adding a string of zeros before and after the pulse (zero padding) because of periodic extension of the pulse implied in the FFT analysis. Figure 1(c) is a counterpart of Figure 1(a) with zero padding and was evaluated for $-1 \leqslant t \leqslant 2$ s in increments of $\Delta t = 1/1000$ s; and the data were subjected to an FFT power spectrum analysis routine available in FLAC. Figure 1(d) shows a plot of the amplitude of FFT power spectrum versus frequencies and is a counterpart of Figure 1(b); results in the two figures compare well.

3.1.3. Interpretation of results. Figures 1(b) and (d) are interpreted to imply the following: There are f/f_0 values for which the amplitude of the FFT power spectrum is zero, i.e. at

$f/f_0 = 0, 2, 3, 4, \ldots$. This implies that frequency spectrum does not contain these frequencies; an alternative interpretation is that for $f/f_0 = 0, 2, 3, 4, \ldots$ values, the sine pulse has zero energy, and therefore, its application to a structure would be inconsequential (not be able to perturb the structure from its prevailing/existing state). The $f/f_0 = 0$ condition is of no interest because f_0 is required to be positive and finite, i.e. $0 < f_0 < \infty$. Thus, for example, the frequency spectrum of a full-cycle sine pulse of 1 s duration ($f_0 = 1$ Hz) has all frequencies except $2, 3, 4, \ldots$ Hz; and application of this sine pulse to a structure would excite all natural frequencies of the structure, except if a natural frequency of the structure happens to coincide with one of these missing frequency values, i.e. $2, 3, 4, \ldots$ Hz. However, this does not pose any difficulty because the frequency spectrum of the excitation pulse can be made to cover the range of frequencies of interest by proper selection of the excitation pulse frequency (f_0). For example, the frequency spectrum of a full-cycle sine pulse with $f_0 = 100$ Hz has frequencies in the ranges between $0, 200, 300, \ldots$ Hz excluding the end values $(0, 200, 300, \ldots)$.

3.2. Natural mode shapes of vibrations

Application of a periodic sinusoidal harmonic force $f(t) = p_0 \sin(\omega_0 t)$ makes the structure oscillate, and in the steady-state vibrations regime, the deformed configuration of the structure is unique to the excitation frequency ω_0. Therefore, for $\omega_0 = \omega_k$, where ω_k is one of the natural frequencies of the structure determined in Section 3.1, the structure's response will be maximum because of resonance, and the steady-state dynamic response will have the kth mode shape. Analytical aspects of this phenomenon are given in text books [4–8]; however, for continuity and completeness of the presentation, analytical aspects of the procedure for a single d.o.f. system are included herein. The analytical details of mode shape for a single d.o.f. system, and a demonstration of extension of these ideas to a multiple d.o.f. system via an example are described below separately.

3.2.1. Analytical formulation for a single d.o.f. system. For dynamic analysis, the governing differential equation of motion is

$$m\ddot{u} + ku = p_0 \sin(\omega_0 t) \tag{7}$$

The solution of Equation (7) is

$$u(t) = A \sin(\omega t) + B \cos(\omega t) + \frac{p_0/k}{1 - (\omega_0^2/\omega^2)} \sin(\omega_0 t) \tag{8}$$

where $\omega = \sqrt{k/m}$.

For the initial conditions $u(0) = \dot{u}(0) = 0$ at $t = 0$, Equation (8) becomes

$$u(t) = \frac{p_0}{k}\left(\frac{1}{1 - (\omega_0^2/\omega^2)}\right)\left[\sin(\omega_0 t) - \frac{\omega_0}{\omega}\sin(\omega t)\right] \tag{9}$$

For $\omega_0 = \omega$, Equation (9) is evaluated in the limit as $\omega_0 \to \omega$ using L'Hôpital's rule and substituting ω for ω_0 in the resulting expression leads to

$$\underset{\omega_0 \to \omega}{Lt}\, u(t) = \frac{-p_0}{2k}[\omega t \cos(\omega t) - \sin(\omega t)] \tag{10}$$

In Equations (7)–(10), entities with subscript 0 refer to the forcing function and those without a subscript refer to the single d.o.f. system.

Figure 2(a) is a plot of Equations (9) and (10) for $p_0/k = 1$ m and $\omega = \pi$ rad/s ($f = 0.5$ Hz) for selected values of $\omega_0 = 0.5\pi$, 1π, 1.5π, and 2π rad/s ($f_0 = 0.25$, 0.5, 0.75, and 1 Hz), i.e. for $\omega_0/\omega = f_0/f = 0.5$, 1.0, 1.5, and 2.0. Equations (9) and (10) are evaluated for $0 \leqslant t \leqslant 5$ s. Plots in Figure 2(a) are intended to show (for a single d.o.f. system): (a) uniqueness of response to harmonic sinusoidal excitations of different frequencies ω_0; (b) comparison of responses for harmonic sinusoidal excitations of different frequencies ω_0, with near-resonant frequency ($\omega_0 \approx \omega$) response dominating all other frequency responses; and (c) displacement amplitude increases in each cycle of the response at resonant frequency. These observations apply equally to systems with multiple degrees-of-freedom as demonstrated below via an example.

3.2.2. Extension to multiple d.o.f. system. Figure 2(b) shows a simply supported beam with three masses, $m_1 = m_2 = m_3 = m$, attached at its quarter points and the beam is assumed to be massless and prismatic with flexural rigidity EI; and this figure also serves as a 2-D model for determination of mode shapes using the proposed procedure. For this problem, the analytical solution for the three natural frequencies of vibrations is [7, 8]: $\omega_1 = 0.7121 \times \lambda$; $\omega_2 = 2.8284 \times \lambda$; and $\omega_3 = 5.9964 \times \lambda$ with $\lambda = \sqrt{48 \times E \times I/m \times l^3}$.

For numerical analyses, the beam is assumed to be 10 m long, 1 m × 1 m in cross section, bulk modulus (K) $= 1 \times 10^8$ Pa, and shear modulus (G) $= 3 \times 10^7$ Pa, $m = 1000$ kg, and density (ρ) of the beam is assigned a value of 1 kg/m^3. For these data, modulus of elasticity (E) $= 8.18 \times 10^7$ Pa, and the analytic values of the natural frequencies from the above formula are: $f_1 = 2.05$ Hz; $f_2 = 8.14$ Hz; and $f_3 = 17.26$ Hz. Three dynamic analyses were made each for $0 \leqslant t \leqslant 2$ s using a periodic sinusoidal harmonic force of each of the three frequency values applied at the centre of mass m_3; and plots of initial configuration of the beam and final deformed grid (magnified) for each of the three natural frequencies are shown in Figure 2(c). The computed mode shapes compare well with those given in Reference [7].

3.2.3. Natural frequencies. For interest, the problem shown in Figure 2(b) was also analysed for determining natural frequency values using the procedure presented in Section 3.1, i.e. by: (a) applying a sinusoidal force pulse of an 100-Hz frequency ($t_0 = 0.01$ s) at the centre of m_3; (b) solving the problem for a $0 \leqslant t \leqslant 2$ s and saving the u-displacement responses at the centres of the three masses; and (c) performing an FFT power spectrum analysis of the time–displacement history data at the centre of m_3. Figure 2(d) shows the example setup for natural frequencies determination using the proposed procedure. The dynamic time step of integration ($\mathrm{d}y\,\mathrm{d}t$) was calculated automatically by the computer program used and its value is 7.47×10^{-6} s. Figure 2(e) shows the u-displacement versus time history at the selected locations; and Figure 2(f) shows the FFT power spectrum results for the displacement–time history data for the centre of the m_3 location. The natural frequencies are estimated (by scaling) to be: $f_1 = 2.04$ Hz; $f_2 = 8.48$ Hz; and $f_3 = 17.08$ Hz; these values compare well with the analytical results.

Results of the example problem give confidence in the viability of the proposed procedure in determining all natural frequencies and associated mode shapes, and the procedure was used with confidence in determining the vibration characteristics for the test problems included in Section 6.

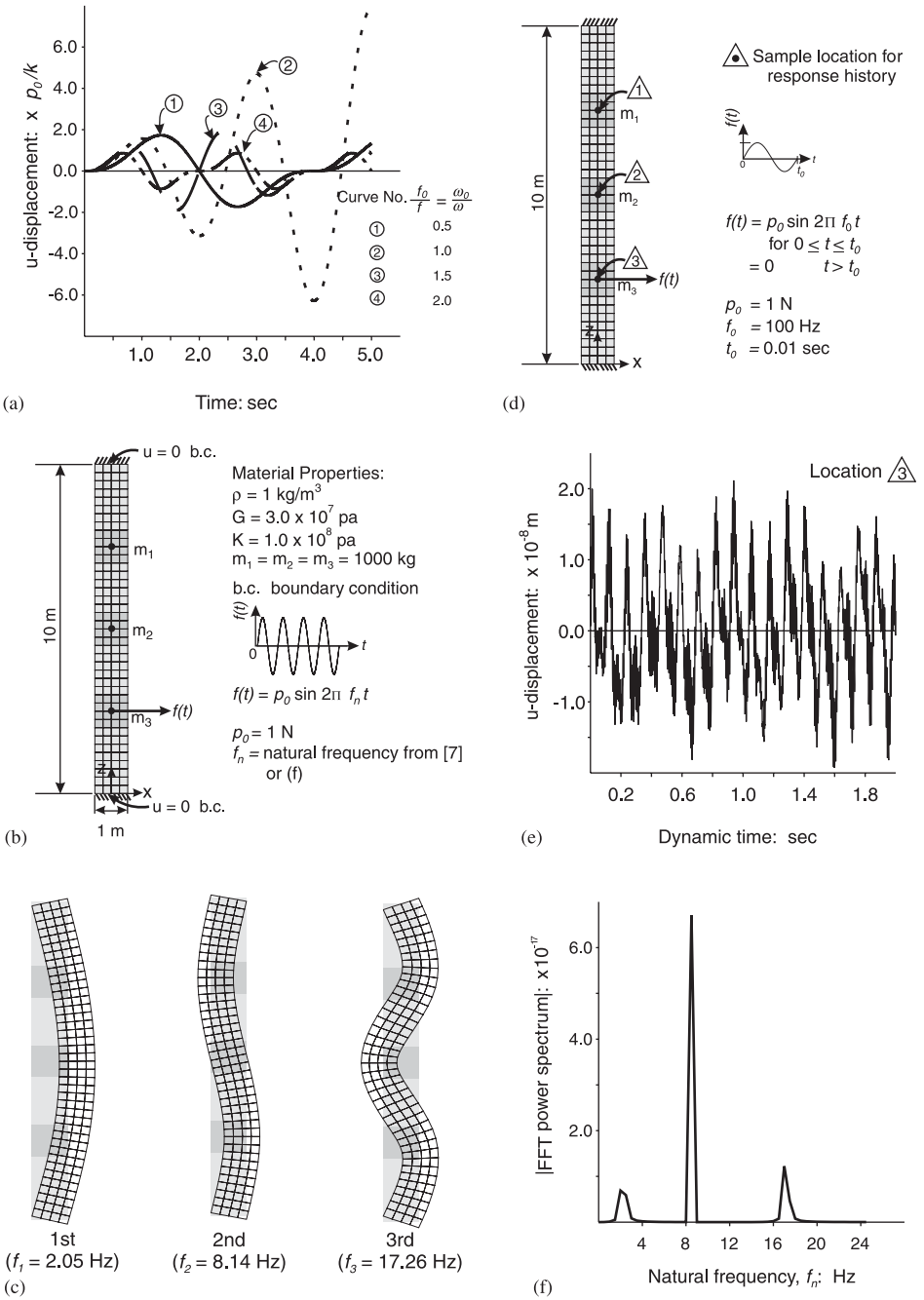

Figure 2. Illustrations for vibration characteristics: (a) displacement responses of a single d.o.f. system using Equations (9) and (10); (b) a simply supported beam with three masses; (c) natural mode shapes (magnified); (d) natural frequencies determination for (b); (e) transverse vibrations; and (f) natural frequencies via FFT power spectrum of (e).

Published in 2006 by John Wiley & Sons, Ltd. *Int. J. Numer. Anal. Meth. Geomech.* 2007; **31**:607–648
DOI: 10.1002/nag

4. EXPECTED RESPONSE CHARACTERISTICS USING THE PROPOSED PROCEDURE

Based on the rationale and details of the proposed procedure described in Sections 2 and 3, a structure subjected to a non-periodic, full-cycle sine pulse force excitation for determination of natural frequencies, and to a periodic sinusoidal force excitation of a natural frequency for mode shape determination shall display the following characteristics in its response:

(a) The structure shall respond to all frequencies in the excitation pulse; however, the amplitudes of responses may differ greatly. The structure's response shall begin to buildup as frequencies in the excitation pulse get closer to one of the structure's natural frequencies, reaching the maximum amplitude when the frequency in the excitation pulse comes closest to the structure's natural frequency value, and then the structure's response shall begin to decline as the frequencies in the excitation pulse get further away from the structure's natural frequency. This sequence of buildup, peak, and decay in the structure's response shall repeat for all its natural frequencies; this sequence shall be evident in the FFT power spectrum plots in the form of wide bases narrowing to sharp spikes along the frequency axis.

(b) The calculated resonant frequency values using the proposed procedure are the natural frequencies of the structure analysed but there is no information on the associated directions of vibrations. This information can be identified from the deformed shape plots. To get a deformed shape, we apply a periodic, sinusoidal force excitation of a natural frequency in one of the co-ordinate directions at an appropriate location on the numerical model; and at the end of dynamic analysis, plot a magnified view of the deformed grid superimposed on the initial undeformed configuration of the model.

(c) In field tests on full-scale structures using mechanical vibrators, response of a structure to a directional disturbance is in all directions; however, magnitude of the response in all directions is not the same because of differences in stiffness. The same shall be true with the results using the proposed procedure. For example, in a 3-D model, if we apply a force pulse in x-direction and record the displacement–time history in x-, y-, and z-directions at a select location on the structure, and afterwards, perform an FFT power spectrum analysis on each of the three displacement–time history data, the frequency content of the three spectra shall be alike, but amplitudes of the FFT power spectra may differ significantly. It may be easier to identify resonant frequencies by examining the FFT power spectrum of the response data in each of the three directions. A resonant frequency is characterized by a decrease in amplitude of the FFT power spectrum of the structure's response data.

5. SELECTION OF PARAMETERS IN THE PROPOSED PROCEDURE

The proposed procedure uses: (a) amplified responses (displacements) of a structure to identify all its natural frequencies that match with the frequencies in the frequency spectrum of the excitation pulse; and (b) the steady-state response (deformed configuration) of the structure to individually periodic wave of each of its natural frequencies to identify the

Published in 2006 by John Wiley & Sons, Ltd. *Int. J. Numer. Anal. Meth. Geomech.* 2007; **31**:607–648
DOI: 10.1002/nag

structure's natural mode shapes. For (a), the time-history of the computed response is converted to a frequency-history using a transform. For (b), the time-domain solution is used. Discretization of a continuum into a finite-difference grid is another important parameter in a numerical model. Selection of the characteristics of the non-periodic pulse, the periodic wave, the transform procedure, and model discretization are described below separately.

5.1. Single pulse excitation function characteristics

Pulse excitations carry a wide range of frequencies, and thus, provide an easy means of disturbing a structure with a frequency-rich perturbation; and all that is left to do is: (a) keeping a record of the time-history of the structure's response at select locations; and (b) analysing the structure's response data to identify the matching frequencies (resonances/spikes). There are a variety of pulse shapes, and their characteristic and analytical details are given in References [4, 5, 7, 8]; however, the information is oriented primarily for studying shock and transient vibrations for objectives such as comparisons of shock motions, design of equipment to withstand shock, simulation of environmental conditions in a laboratory, etc. For the work reported in this paper, only a full-cycle sinusoidal pulse was used and no attempt was made to use other pulse shapes. Advantages in using a full-cycle sine pulse include: (a) an accurate implementation with relative ease in the numerical solution scheme because of smoothness of the sine-function; and (b) the integral of a full-cycle sine pulse is zero, i.e. it does not add any energy to the system, and the vibration is the continuing result of the initial disturbance. Considerations for details of a full-cycle sine pulse for the objectives of this paper include:

(a) The frequency of the excitation pulse (ω_0 or f_0) can be estimated knowing the highest value of natural frequency ($\omega_n|_{\max}$ or $f_n|_{\max}$) of interest for the structure under study. Ideally, f_0 can be one-half of $f_n|_{\max}$; however, for increased coverage of the range of computed natural frequency values by the use of the proposed procedure, it is suggested to use $f_0 = f_n|_{\max}$. It may be desirable to repeat the dynamic analysis of a problem by defining the dynamic time-step at successively smaller values and evaluating the frequency results for consistency in the computed frequency values. For all problems included in this paper, a full-cycle sine pulse excitation of $f_0 = 100$ Hz ($t_0 = 0.01$ s) was used; the dynamic time-step size was selected by FLAC and was typically of the order of 10^{-5}–10^{-6} s.
(b) The duration of dynamic analysis (dyt) should always be greater than the duration of the excitation pulse (t_0); however there is no constraint on a higher value for dyt. It is essential to have a good representation of the steady-state response in the time-history data, and a plot of displacement versus dynamic time can be examined visually to see the repeat of steady-state response. However, with the use of efficient personal computers, duration of dynamic analysis is not likely to be a concern. For the example problem in Section 3, dyt = 2 s; for the test problems in Section 6, dyt = 5 s; and for the sample problem in Section 6, dyt = 0.5 s were used.

5.2. Periodic excitation function characteristics

The excitation function for determining mode shapes associated with natural vibration frequencies is a periodic sinusoidal force, and the frequency of the sine wave is set equal to the natural frequency of vibration for which the mode shape is desired. The duration of the periodic force function is equal to the duration of the dynamic analysis (dyt). The minimum value for dyt

depends on the frequency of the sine wave and the material properties and physical dimensions of the numerical model; however, there is no constraint on a higher value for dyt. Once a few cycles of the sine pulse have travelled the model, the steady-state deformed configuration of the structure is established. For the example problem in Section 3, dyt = 2 s; for the test problems in Section 6, dyt = 5 s; and for the sample problem in Section 6, dyt = 0.5–1.5 s (depending on the natural frequency) were used.

5.3. *Transform*

In civil engineering, Fourier transform is usually used to relate an event in time domain $f(t)$ to the same event in frequency domain $F(\omega)$; continuing its use for the objectives of this paper is suggested. The FFT power spectrum routine included in Reference [2] was used for all FFT analyses results included in this paper.

5.4. *Model discretization*

In general, a discretization (grid size) of a continuum that is appropriate for dynamic analysis can be used to determine natural vibration characteristics using the proposed procedure. General guidance on grid size for dynamic analysis is to keep the spatial grid size to be smaller than about one-tenth of the wavelength associated with the highest frequency component of the excitation wave [2].

6. TEST PROBLEMS

Three test problems are used to check the validity of the proposed procedure and accuracy of results from its use. Test problems are: (a) a cantilever beam, (b) a two-span beam with simply supported ends, and (c) a concrete gravity dam. The numerical solutions for the vibration characteristics were obtained using FLAC [2]. The following outline is followed for each of the test problems:

(a) The continuum of the test problem is discretized into a finite-difference grid of suitable spacing (appropriate for dynamic analysis of the problem). Physical boundary conditions of the problem are imposed on the numerical model.
(b) For determination of natural frequencies of vibration, the excitation function ($f(t) = p_0 \sin(2\pi f_0 t)$ for $0 \leqslant t \leqslant t_0$ and $f(t) = 0$ for $t > t_0$, where $t_0 = 1/f_0$) is a pulse force and is applied at one of the locations in the discretized model of the problem in the x-direction, and the problem is analysed for a time duration $t =$ dyt; displacement–time histories at select locations are saved. At the end of the dynamic analysis, an FFT power spectrum analysis is performed on one or more of the displacement–time history data sets, and the results of frequency versus amplitude of the power spectrum are plotted. Frequencies corresponding to the sharp spikes in the amplitude of the FFT power spectrum are read off from the frequency–amplitude plot; these frequencies are interpreted to represent the natural frequencies of vibrations of the problem; the lowest frequency value corresponds to the first natural frequency (fundamental frequency) of the problem analysed, with each higher frequency value corresponding to the next higher (2nd, 3rd, ... *Nth*) natural frequency of vibration of the problem analysed.

(c) For determination of mode shape corresponding to each natural frequency of vibration, the excitation function ($f(t) = p_0 \times \sin(2\pi \times$ natural frequency $\times\, t)$ for $0 \leqslant t \leqslant$ dyt) is a force and is applied at one of the locations in the discretized model of the problem in the x-direction and the dynamic analysis performed for a time duration $t =$ dyt. At the end of each analysis, the initial undeformed configuration of the model and a magnified view of the deformed grid of the model are plotted. The deformed grid is interpreted to represent the mode shape corresponding to the natural frequency value used.

(d) For determination of direction of vibration (transverse, vertical, longitudinal, or rotational) associated with a natural frequency, the deformed configuration of the structure is examined.

6.1. Test problem no. 1—a cantilever beam

This test problem has analytical solutions for natural frequencies and mode shapes listed in Reference [5]; however, the frequency values listed have implicit assumptions that only bending stresses contribute to beam deflection and that during transverse vibrations, each element of the beam moves in the transverse direction without rotation (classical theory). However, in the beam theory, the assumptions are that shear stresses contribute to beam deflection, and that each plane section that is initially normal to the axis of the beam remains plane and normal to the axis during deflection. Thus, for comparison of numerical results using the proposed procedure, the analytical natural frequency values were corrected for rotary inertia and shear deformations. Figure 3 shows the rotary inertia and shear force correction factors for natural frequencies of uniform cantilever beams [5, 9]. Figure 3 is reproduced with permission of the McGraw-Hill Companies.

The cantilever beam for the test problem is assumed to be 10 m long, and 1 m × 1 m in cross section. The material properties used are: density (ρ) = 1000 kg/m^3, bulk modulus (K) =

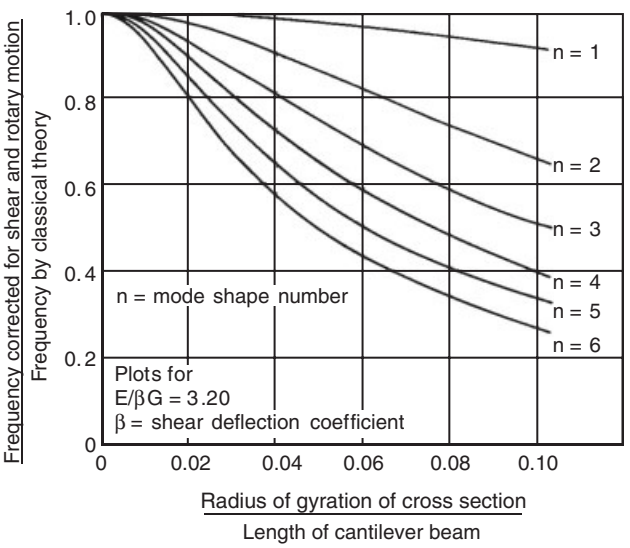

Figure 3. Influence of shear force and rotary motion on natural frequencies of uniform cantilever beams [5, 9]—reproduced with permission of the McGraw-Hill Companies.

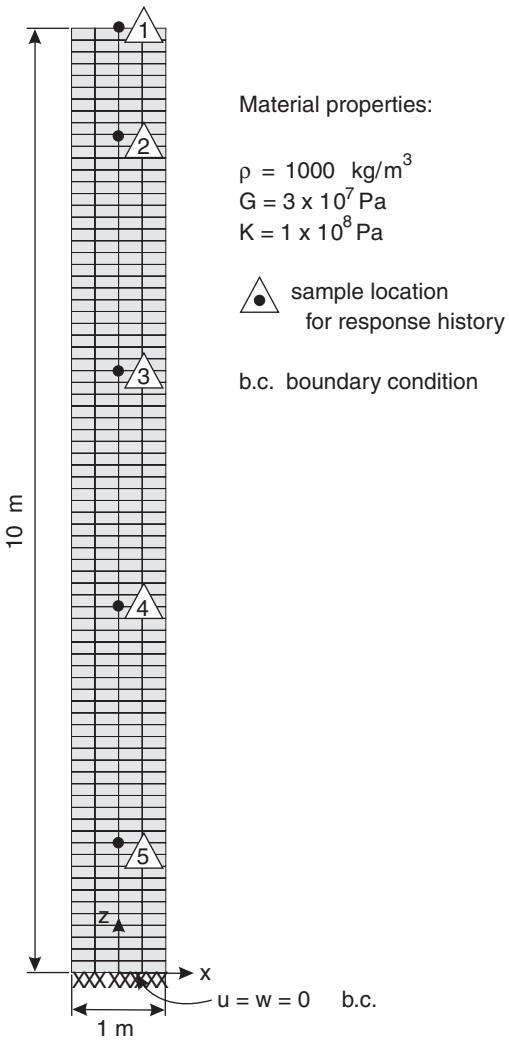

Figure 4. Test problem no. 1—natural vibration characteristics of a cantilever beam.

1×10^8 Pa, and shear modulus $(G) = 3 \times 10^7$ Pa; the corresponding value of modulus of elasticity $(E) = 8.18 \times 10^7$ Pa. Figure 4 shows the test problem; this figure also serves as a 2-D model of the test problem for analyses using the proposed procedure.

Figure 5(a) shows the setup of the FLAC model of the test problem. It is divided into a 4×80 grid. The base is fixed with $u = w = 0$ boundary conditions. The excitation force is a single sine pulse of 100 Hz applied at the centre of the free end of the cantilever beam, and the problem is solved for dyt = 5 s. The dynamic–time step of integration used is 1.494×10^{-4} s. Figure 5(b) shows the displacement–time response at the selected location. Figure 5(c) shows the FFT power spectrum of the data shown in Figure 5(b)—the plot shown is limited to display results for up to the first five natural frequencies for which results are given in Reference [5]. The sharp spikes in

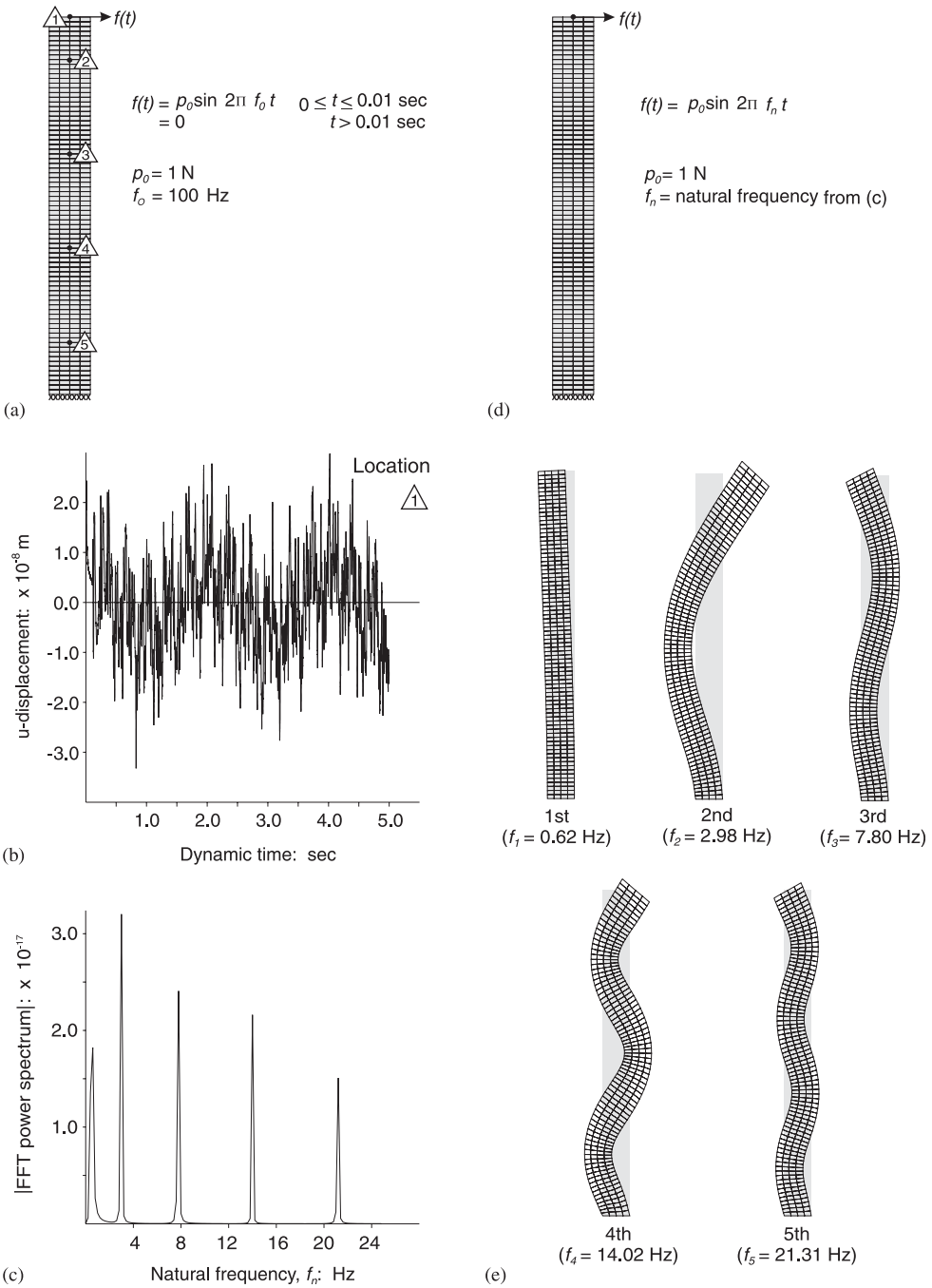

Figure 5. Natural vibration characteristics of test problem no. 1 (Figure 4): (a) problem setup for natural frequencies determination; (b) transverse vibrations; (c) natural frequencies via FFT power spectrum of (b); (d) problem setup for mode shape determination; and (e) natural mode shapes (magnified).

the FFT power spectrum are interpreted to represent resonances occurring at natural frequencies of the cantilever beam. The first five natural frequencies of free vibrations in the transverse direction are estimated (by scaling from Figure 5(c) plot) at: 0.62, 2.98, 7.80, 14.02, and 21.31 Hz, respectively. Figure 5(d) shows the setup of FLAC model for natural mode shapes determination. The excitation force is a periodic sine wave of selected natural frequency for which the mode shape is desired. The mode shapes corresponding to the computed natural frequencies are shown in Figure 5(e). Note that plane sections that were initially normal to the axis of the beam remained normal to the axis during transverse vibrations.

The analytic solutions for the first five natural frequencies for transverse vibrations listed in Reference [5] are 0.46, 2.92, 8.11, 15.89, and 26.26 Hz. Corrections for rotary motion and shear force effects were estimated from Figure 3. For the test problem, the correction factors are estimated at 1.0, 0.950, 0.875, 0.822, and 0.756 for the first through fifth natural frequency values and correspond to the value of 0.0289 for the x-axis entity in Figure 3. These correction factors are used as multipliers to the listed values (0.46, 2.92, 8.11, 15.89, and 26.26, respectively). Thus, the corrected values of analytic results (for comparison with the numerical model results) are 0.46, 2.77, 7.10, 13.06, and 19.85 Hz.

The natural frequency values resulting from application of the proposed procedure compare well with those obtained from the values given in the literature (after correction for shear force and rotary motion). The numerical model results are a little higher than their analytical counterparts. The mode shapes shown in Figures 5(e) compare well with those given in Reference [5].

6.2. Test problem no. 2—a two span beam with simply supported ends

For this test problem, it is known that the symmetric deflected shape under the beam's own weight is not appropriate for computing the lowest natural frequency because the fundamental frequency is associated with an antisymmetric mode shape [4]. The proposed procedure is used to compare its results with those given in Reference [5].

The two-span beam is assumed to be 20 m long (each span length = 10 m) with simply supported ends and 1 m × 1 m in cross section. The material properties used are: density $(\rho) = 1000\ \text{kg/m}^3$, bulk modulus $(K) = 1 \times 10^8$ Pa, and shear modulus $(G) = 3 \times 10^7$ Pa. Figure 6 shows the test problem; and this figure also serves as a 2-D model of the test problem for analyses using the proposed procedure.

Figure 7(a) shows the setup of the FLAC model of the test problem. It is divided into a 4×80 grid. The two end supports and one in the middle of the beam are assigned the $u = 0$ boundary condition. The excitation force is a single sine pulse of 100 Hz and is applied at ($x = 0$, $z = 19.75$ m) location—this location is the first interior grid point from the end-support B; and the problem is solved for dyt = 5 s. The dynamic time step of integration used is 2.362×10^{-4} s. Figure 7(b) shows the displacement–time history at the selected location. Figure 7(c) shows the FFT power spectrum of the data shown in Figure 7(b). The first five natural frequencies of free vibrations in the transverse direction are estimated (by scaling from Figure 7(c) plot) at 1.42, 2.19, 5.41, 6.59, and 11.20 Hz, respectively. Figure 7(d) shows the setup of FLAC model for natural mode shapes determination. The excitation force is a periodic sine wave of selected natural frequency for which the mode shape is desired. The mode shapes corresponding to the computed natural frequencies are shown in Figure 7(e).

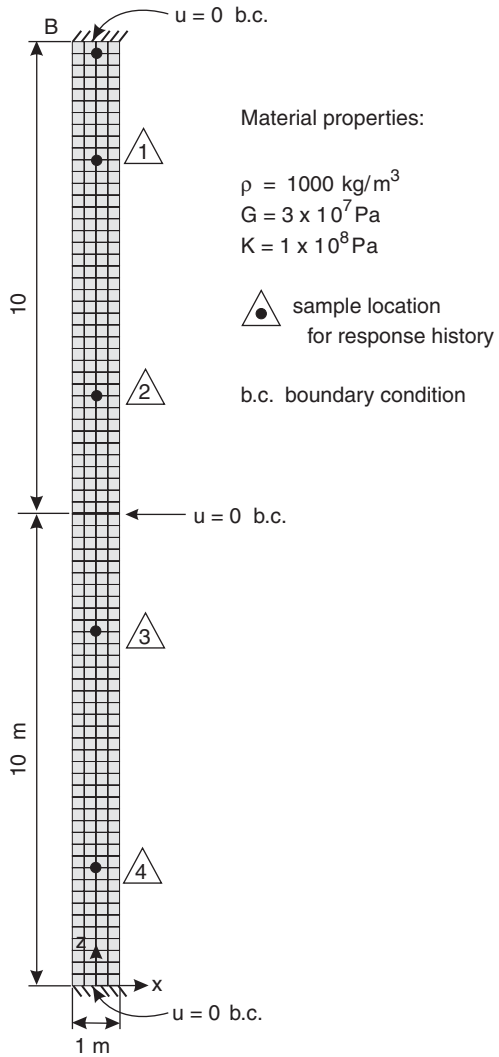

Figure 6. Test problem no. 2—natural vibration characteristics of a two-span beam.

The analytic solutions for the first five natural frequencies for transverse vibrations are [5]: 1.30, 2.02, 5.19, 6.55, and 11.67 Hz. The frequency and mode shape results from application of the proposed procedure compare well with the known analytical results.

6.3. Test problem 3—concrete gravity dam

For this test problem, field tests using mechanical vibration generators were performed to determine natural vibration characteristics. As a part of the field test program, two- and three-dimensional finite element numerical models of the dam were also analysed to compare results. Details of the field test, site conditions, and discussions of results from tests and numerical

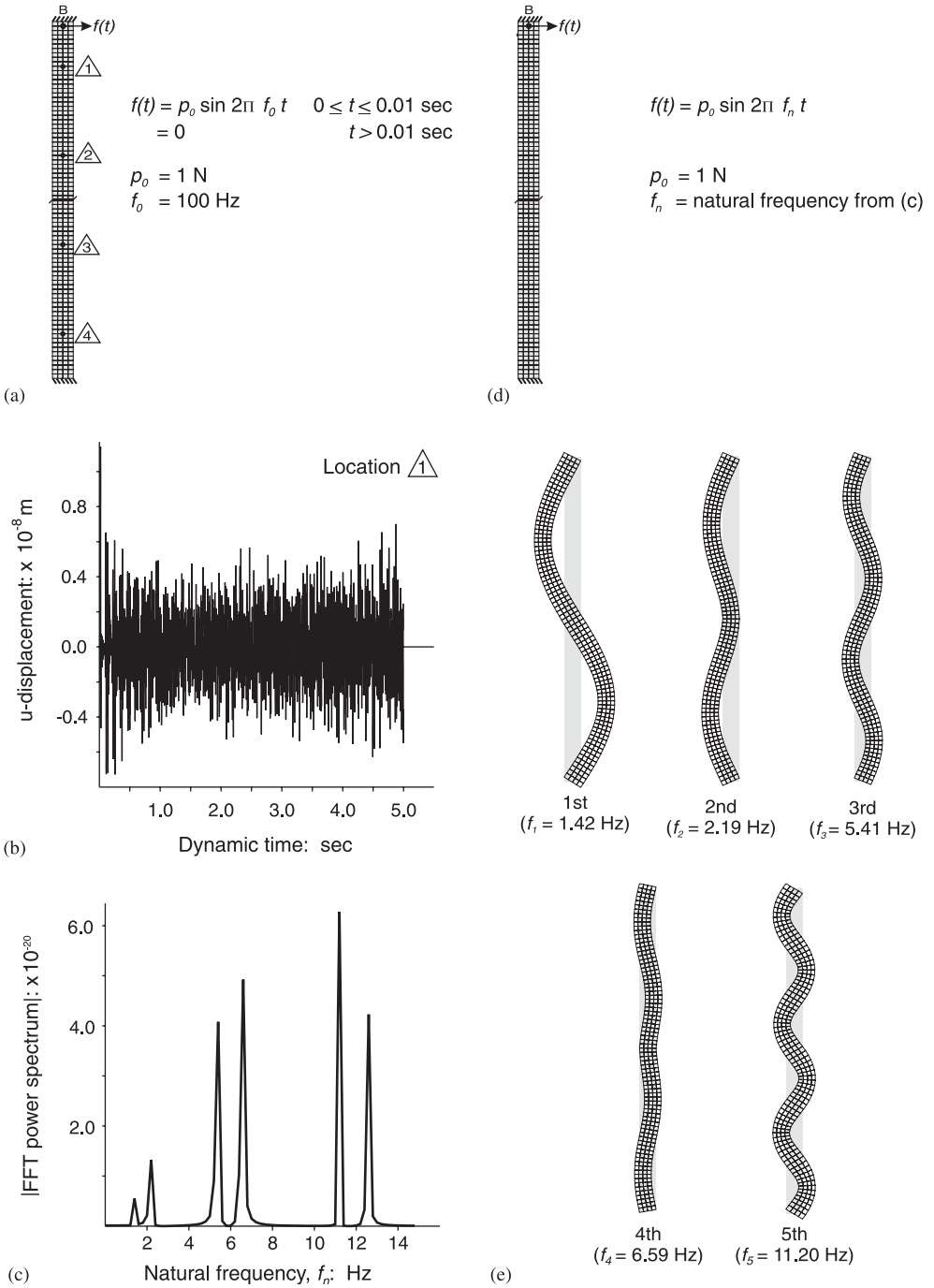

Figure 7. Natural vibration characteristics of test problem no. 2 (Figure 6): (a) problem setup for natural frequencies determination; (b) transverse vibrations; (c) natural frequencies via FFT power spectrum of (b); (d) problem setup for mode shape determination; and (e) natural mode shapes (magnified).

Published in 2006 by John Wiley & Sons, Ltd. *Int. J. Numer. Anal. Meth. Geomech.* 2007; **31**:607–648
DOI: 10.1002/nag

models are given in Reference [10]; only pertinent details related to winter tests are included herein.

6.3.1. Field test and site conditions. Figure 8 shows the cross section of a concrete gravity dam through one of its construction blocks (monoliths) located approximately midway between the abutments. The dam is 121.92 m high and 560.83 m long, has 37 monoliths of varying height, and had winter reservoir water storage during the field tests. The dam was vibrated by means of two eccentric-mass vibration generators attached to the crest of the dam on one of the monoliths (cross section similar to the one shown in Figure 8) near the centre of the dam. The two machines were located close together in order to apply essentially a single horizontal force at the centreline of the monolith. Acceleration response of the dam was achieved by increasing in steps the frequency of rotation of the vibration generators from 1 to 8 Hz. At each step, the excitation frequency was held constant until steady-state vibrations were achieved, and then the response of the dam and the frequency of excitation were recorded. Resonant frequencies identified from the field data are 3.47, 4.13, 5.40, 6.10, 6.50, and 7.47 Hz. The crest and vertical mode shapes of the dam were determined by vibrating the dam at each resonant frequency in turn and

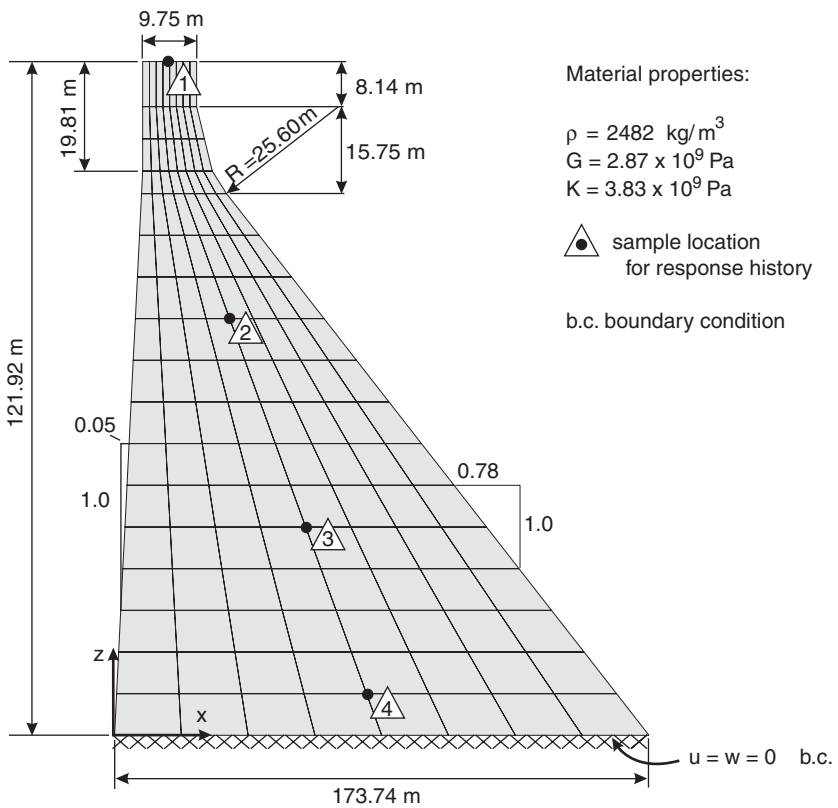

Figure 8. Test problem no. 3—natural vibration characteristics of a concrete gravity dam.

measuring the acceleration amplitudes at various points along the length and height of the dam. Plots of the crest mode shapes showed that the resonant frequencies identified above corresponded to modes 1, 2, 4, 5, 6, and 8; the third and seventh modes did not get excited, which indicated that both of these crest modes have a stationary point located at the block where the vibration generators were placed. The frequency values from the field test are shown in Table I.

6.3.1.1. Dynamic analyses. Dynamic analyses of the dam included: (a) a three-dimensional (3-D) finite element model, and (b) a two-dimensional (2-D) finite element model. The 3-D model did not include the reservoir; 2-D models were with and without the reservoir. Analysis results included herein were without the reservoir.

Figure 8 also serves as the 2-D finite element model of the dam. The material properties for concrete in the dam are: density (ρ) = 2482 kg/m^3, elastic modulus (E) = 6.89×10^9 Pa, and Poisson's ratio (υ) = 0.2. The value of E used in analyses was for convenience (due to lack of a definite value). Since mode shapes are independent of the value of E, and natural frequencies are proportional to $\sqrt{E}$, the frequency values from the numerical model(s) were multiplied by a scale factor $\alpha = \sqrt{E_{\text{effective}}/E_{\text{assumed}}}$. The Rayleigh–Ritz procedure was used to determine natural frequencies and mode shapes. From the results of vibration tests, finite element analyses, and other considerations, $E_{\text{effective}} = 2.24 \times 10^{10}$ Pa was estimated for concrete in the dam; this gives $\alpha = 1.80$. The adjusted frequency values for the first two modes of vibrations are: $f_1 = 3.14$ Hz and $f_2 = 5.19$ Hz, and the corresponding mode shapes shown are typical of x-direction vibrations of a cantilever beam. There is uncertainty expressed about the validity of the computed $f_2 = 5.19$ Hz based on comparisons of mode shapes from 2-D and 3-D analyses, and a preference is indicated for $f_2 = 8.17$ Hz which is the f_6 from the 3-D model results. Thus $f_1 = 3.14$ Hz and the associated mode shape are the only definite results from the 2-D model analyses included in Reference [10]. The other significant comment is that a 2-D model is not an adequate representation of the prototype and that a 3-D model with inclusion of the reservoir water is more appropriate for determining dynamic properties of the dam. However, the computed values of natural frequencies from the 3-D and 2-D models are included in Table I.

6.3.2. Proposed procedure. Figure 8 also serves as a 2-D model of the test problem for analyses using the proposed procedure. The material properties used are: density (ρ) = 2482 kg/m^3, shear modulus (G) = 2.87×10^9 Pa, and bulk modulus (K) = 3.83×10^9 Pa (G and K values correspond to $E = 6.89 \times 10^9$ Pa and $\upsilon = 0.2$ used in Section 6.3.1.1).

Table I. Test problem no. 3—comparison of results (Hz).

	Frequency of natural vibration, Hz							
Source	1st	2nd	3rd	4th	5th	6th	7th	8th
Field test	3.47	4.13	—	5.40	6.10	6.50	—	7.47
3-D FEM	3.70	4.43	4.89	5.66	6.30	8.17	—	—
2-D FEM	3.14	5.19	—	—	—	—	—	—
FLAC (Figure 9)	3.24	6.87	9.03	11.86	17.60	19.43	24.46	26.28

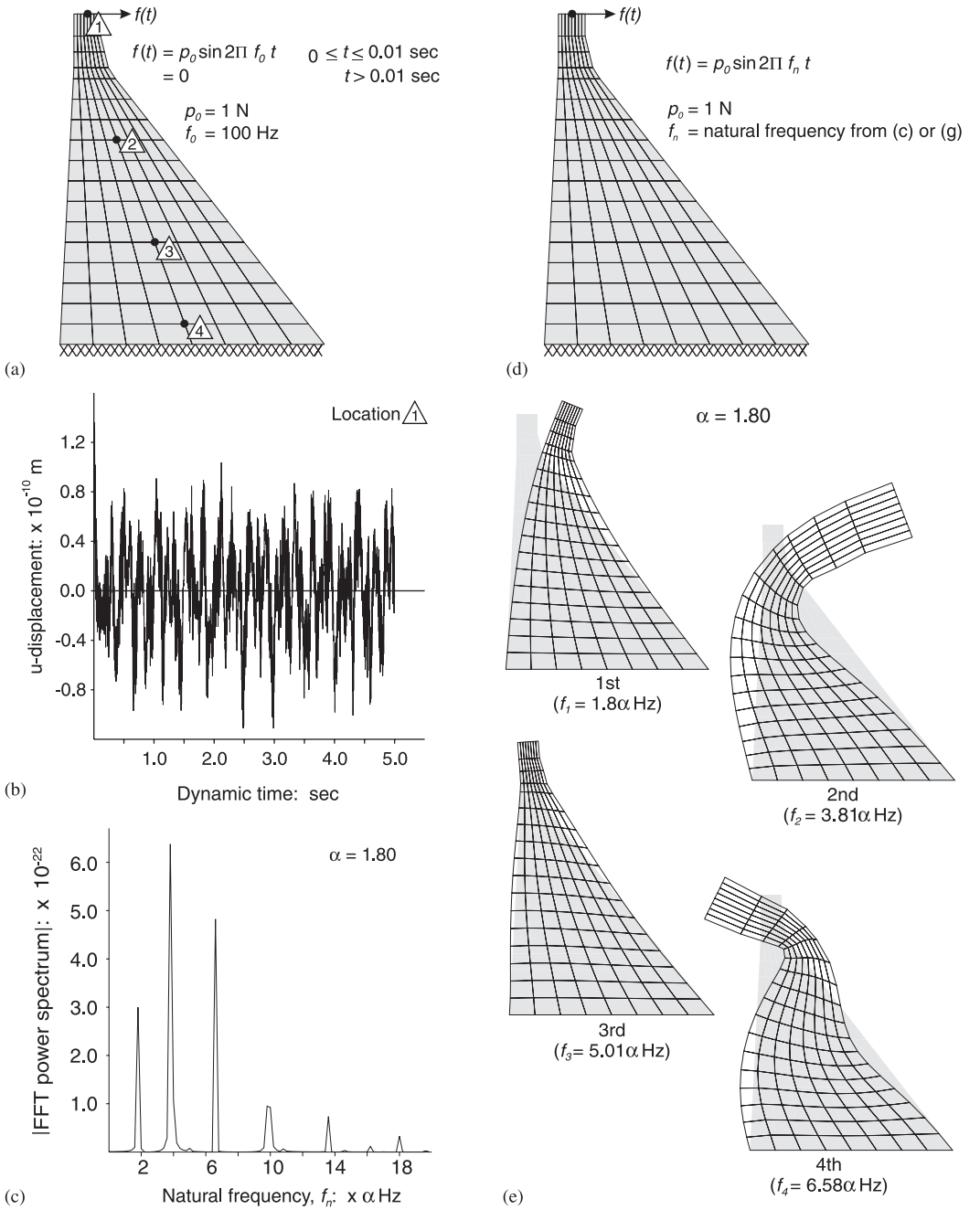

Figure 9. Natural vibration characteristics of test problem no. 3 (Figure 8): (a) problem setup for natural frequencies determination; (b) transverse vibrations; (c) natural frequencies via FFT power spectrum of (b); (d) problem setup for mode shape determination; (e) natural mode shapes (magnified); (f) vertical vibrations; and (g) natural frequencies via FFT power spectrum of (f).

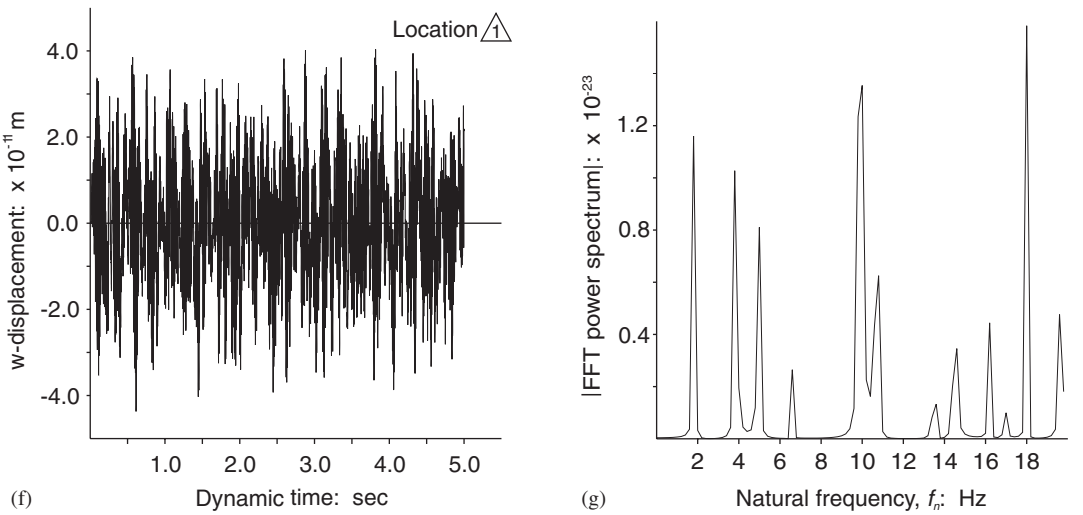

Figure 9. *Continued.*

Figure 9(a) shows the setup of the FLAC model of the test problem. The continuum is divided into an 8×17 grid (the same as used for the 2-D model in Reference [10]). The base of the model is fixed with $u = w = 0$ boundary conditions. The excitation force is a single sine pulse of 100 Hz and is applied at the centre of the dam crest; and the problem is analysed for dyt = 5 s. The dynamic time step of integration used is 3.432×10^{-4} s. Figure 9(b) shows the u-displacement versus time history at the selected observation location. Figure 9(c) shows the FFT power spectrum of the data shown in Figure 9(b)—the plot is limited to all resonating frequencies up to 20 Hz, and the estimated values for the first eight resonating frequencies are: 1.80, 3.81, 5.01, 6.58, 9.76, 10.78, 13.57, and 14.58 Hz (these values are multiplied by the scale factor $\alpha = 1.80$ to get applicable values for the dam shown in Table I). In Figure 9(c), the resonances corresponding to frequency values of 5.01, 10.78, and 14.58 are relatively weak, but they are counted as indicative of natural frequencies. Figure 9(d) shows the setup of the FLAC model for natural mode shapes determination. The mode shapes associated with the first four natural frequencies are shown in Figure 9(e), other mode shapes are not included to conserve space.

Figure 9(f) shows the w-displacement versus time history at the same location and in the same analysis for which u-displacement versus time history is shown in Figure 9(b). Figure 9(g) shows the FFT power spectrum of the response data shown in Figure 9(f). It is easier to identify resonances at frequency values of 5.01, 10.78, and 14.58 in Figure 9(g) as compared to Figure 9(c).

6.3.2.1. Comparison of results. Table I shows the resonant/natural frequency values determined from the field test (with winter reservoir water storage), 3-D and 2-D finite element model analyses (without reservoir water), and the results from the proposed procedure. For the conditions included in the FLAC model, only results from the 2-D finite element model without the reservoir are of direct use in comparing results using the proposed procedure.

(a) The first two frequency values compare as: $f_1 = 3.24$; $f_2 = 6.87$ Hz by the proposed procedure versus 3.14 and 5.19 or $f_6 = 8.17$ (from the 3-D model) Hz given in Reference [10]; the corresponding mode shapes compare well. These results are taken to indicate good agreement.
(b) For higher modes of vibrations, 2-D results are not given in Reference [10]. Compared to the 3-D FEM results, the proposed procedure frequency values for higher modes are significantly higher. In principle, this agrees with the qualitative observations leading to the conclusion that a 2-D model is not appropriate for this example problem [10].
(c) The mode shapes associated with the higher frequency values using the proposed procedure have reasonable appearances. From the deformed configuration of the dam, Figure 9(e), $f_3 = 5.01\alpha$ appears to be associated with vertical mode of vibration.
(d) The problem shown in Figure 8 was also solved using 16×34; 24×51; 32×68; and 40×85 grid, and sine pulse of different frequencies, but the FFT results did not change significantly.
(e) A 3-D analysis using the proposed procedure was not performed due to lack of sufficient information in Reference [10] for developing a FLAC3D model of the dam.

7. SAMPLE PROBLEM

Figure 10 shows a 3-D view of a typical panel of the prototype spillway control structure located near the abutment end of an embankment dam. The spillway is a gated facility with two side-walls, two intermediary piers (three radial gates), and a bridge deck and is located along the curved portion of the dam axis. The side-walls are counterforted and have vertical inside faces

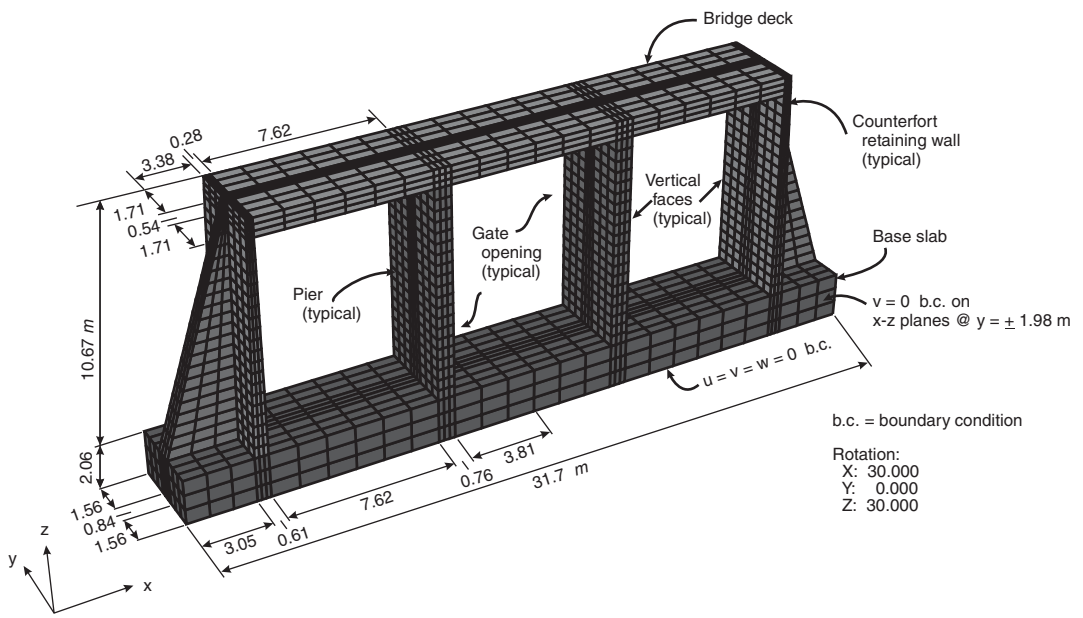

Figure 10. Sample problem—natural vibration characteristics of a spillway control structure without the embankment materials.

(for gates). The bridge deck shown in Figure 10 is an equivalent rectangular slab of the same overall geometric dimensions as the prototype (T-beam construction) and was assigned a reduced density value to preserve the overall mass of the prototype bridge structure in the numerical model(s). Thus, the side-walls are non-symmetric and non-prismatic; the piers, bridge deck, and base slab are symmetric and prismatic. The control structure is founded on compacted embankment fill; and the embankment fill is compacted against the two side-walls. Normal to the spillway centreline, looking in the downstream direction, there is a natural hillside to the left and sloping face of the dam and the underlying rock formations to the right.

Dimensions of various components of the prototype control structure modelled are shown in Figure 10. In brief, the spillway control structure is 31.70 m wide (x-direction) by 12.73 m high (z-direction), and the length (y-direction) of one panel is 3.96 m. The base slab is 2.06 m thick and the bridge deck is 0.84 m thick. The piers are 0.76 m wide by 9.83 m high. The side-walls are 10.67 m high counterfort retaining walls with stem width of 0.61 m at the base tapering to 0.28 m at the top, and the counterforts are 3.05 m long (x-direction) at the base and taper to zero at the top, and 0.84 m wide (y-direction) at the base and taper to 0.54 m at the top. The embankment modelled is 277.37 m wide (x-direction) by 85.34 m high (z-direction) on the left (hill side) and 50.09 m high on the right (embankment side), and 3.96 m long (y-direction).

Estimated values for the material property parameters (ρ, G, and K) for the reinforced concrete and the geo-materials are shown in Table II. There are 3 interfaces—one along the contact between the base-slab and the embankment fill; and two along the vertical planes located at the ends of the base slab. The interface properties for the interfaces along the vertical planes are assumed to be the same. The normal and shear stiffness values along the interfaces are assigned the following values:

Base-slab—embankment soil contact: $k_n = 4.2 \times 10^8$ Pa/m; $k_s = 6.0 \times 10^7$ Pa/m
Side wall soil—embankment soil contact: $k_n = 2.1 \times 10^8$ Pa/m; $k_s = 1.5 \times 10^7$ Pa/m

All interfaces were considered glued (no slip or separation allowed along the interfaces).

For the objectives of this paper, the analysis details/results for the following four model conditions are included:

(a) A limited 3-D model of the prototype structure; limitations include: (i) only one panel length of the complete spillway control structure is considered; (ii) embankment fill

Table II. Sample problem—material properties.

Material identifier	Density (ρ) (kg/m^3)	Elastic constants	
		Bulk modulus (K) (GPa)	Shear modulus (G) (GPa)
Reinforced concrete	2400	16.0	14.5
Embankment fill	2080	0.41	0.21
Sandstone	2500	27.0	7.0
Shale	2400	7.0	4.0
Rock	2600	13.0	8.0

Unit weight = density × gravity.

against the counterforted walls is excluded; and (iii) the control structure is assumed fixed at the base slab. Figure 10 shows the details of the 3-D model. Analysis details and results included are just like those for the test problems.

(b) An equivalent 2-D model of the prototype spillway panel included in (a). In the 2-D equivalent model, the counterforted walls are replaced by equivalent cantilever walls using the procedure presented in Reference [1]. The equivalent cantilever wall is 1.26 m wide at the base and tapers to 0.28 m at the top; the elastic constants (G and K) are χ times the corresponding values for reinforced concrete shown in Table II—the multiplier $\chi = 16.2$ at the base of the wall and varies linearly to a value of $\chi = 1$ at the top of the wall. The layout and overall dimensions of the concrete structure are maintained in the equivalent 2-D model, i.e. the equivalent cantilever wall is assigned a vertical face coincident with the vertical face of the prototype counterfort retaining wall; thus, the dimension of the overhang of the base-slab past the embankment-side of the side-walls (3.05 m) gets reduced to 2.40 m in the equivalent model. The equivalent section of the bridge deck is 0.84 m thick slab and the density of the equivalent deck is 1120 kg/m^3. All else (except for the dimensionality) is the same as for the 3-D model of the prototype structure. Figure 12 shows the details of the 2-D equivalent model. Analysis details and results included are just like those for (a).

(c) A 3-D model for one panel length of the prototype structure, i.e. geo-materials plus the prototype control structure. Figure 14 shows the details of the 3-D model. Analysis details and results included are just like those for (a).

(d) A 2-D model of the prototype structure with equivalent cantilever side-walls, i.e. geo-materials plus the equivalent control structure. Figure 16 shows the details of the 2-D model. Analysis details and results included are just like those for (b).

There are no known solution(s) for natural frequencies or mode shapes for this problem with or without the geo-materials; therefore, results of 3-D and 2-D model studies using the proposed procedure are compared among themselves; first natural frequency and mode shape results for the 3-D and 2-D models using the alternative procedure are included in Appendix A.

7.1. Spillway control structure without the embankment fill

7.1.1. 3-D model. Figure 10 also serves as a 3-D model for determination of natural vibration characteristics. This may be considered as a hypothetical condition as it does not represent a field condition. Figure 11(a) shows the problem setup for FLAC3D analysis using the proposed procedure.

The excitation force is a single sine pulse of 100 Hz and is applied at the point of complete symmetry in the x- and y-co-ordinate directions; and the problem is analysed for dyt = 0.5 s. The dynamic time step of integration used is 1.995×10^{-6} s. Figure 11(b) shows the displacement–time history at the base of the pier location; this response history gave the clearest FFT power spectrum shown in Figure 11(c). Results of the first five natural frequencies determined by scaling Figure 11(c) are included in Table III. Figure 11(d) shows the problem setup for mode shapes determination. Figure 11(e) shows the mode shapes for the first three natural frequencies.

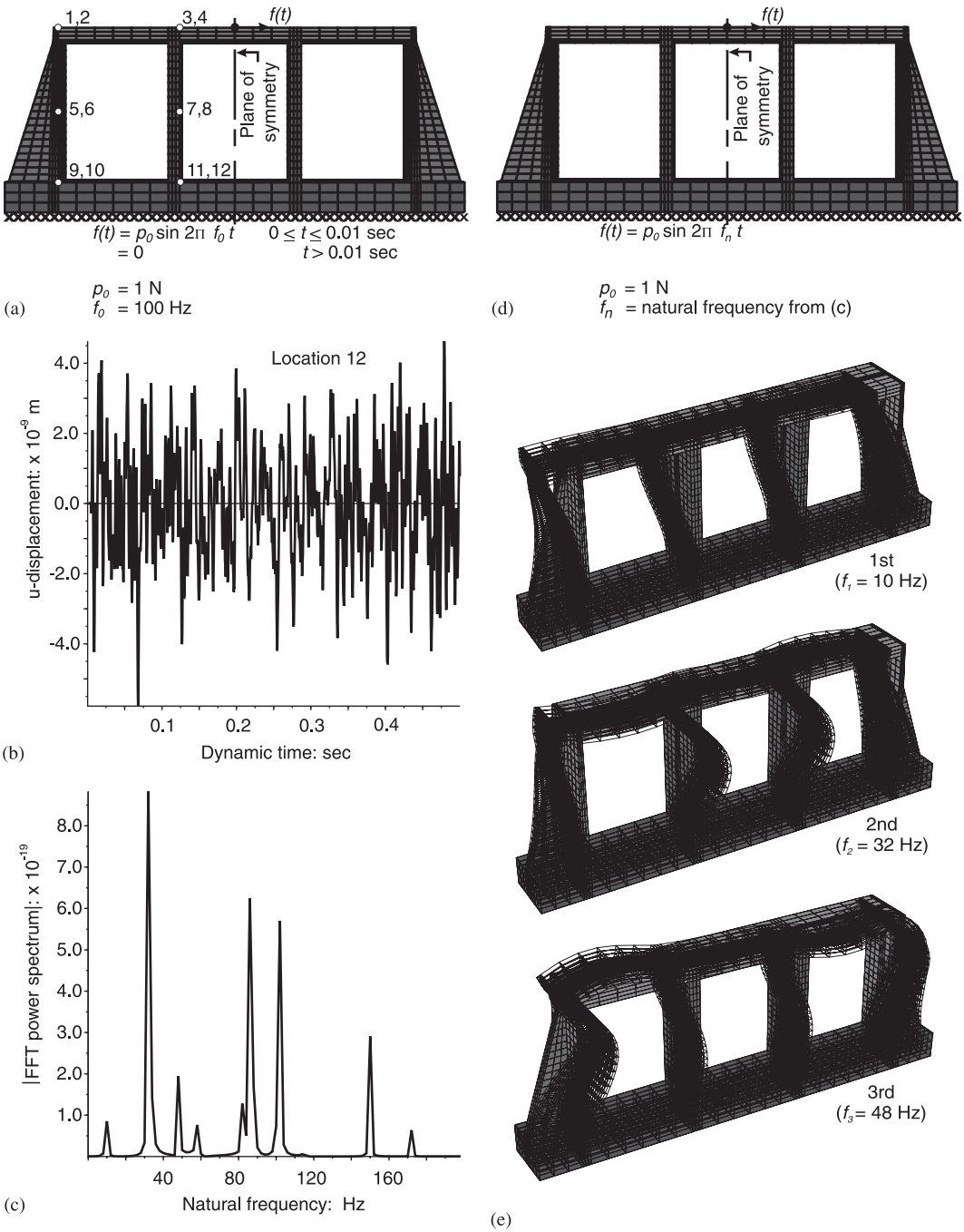

Figure 11. Natural vibrations characteristics of sample problem using the 3-D model (Figure 10): (a) problem setup for natural frequencies determination; (b) transverse vibrations; (c) natural frequencies via FFT power spectrum of (b); (d) problem setup for mode shape determination; and (e) natural mode shapes (magnified).

Published in 2006 by John Wiley & Sons, Ltd. *Int. J. Numer. Anal. Meth. Geomech.* 2007; **31**:607–648
DOI: 10.1002/nag

Table III. Sample problem—comparison of results (Hz).

Model condition	Proposed procedure									
	3-D model					2-D equivalent model				
	1st	2nd	3rd	4th	5th	1st	2nd	3rd	4th	5th
Without fill	10.0	32.0	48.0	58.0	82.0	14.0	40.0	74.0	80.0	102.0
With fill	4.0	8.0	11.8	17.8	21.8	3.8	8.0	11.8	18.0	22.0

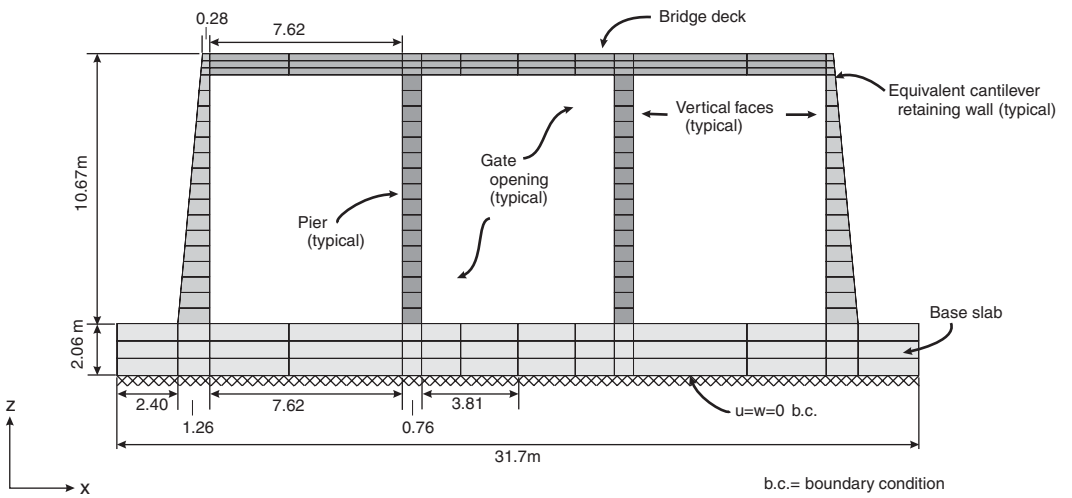

Figure 12. Equivalent 2-D model of sample problem (Figure 10).

7.1.2. 2-D model. Figure 12 shows the equivalent 2-D model of the prototype panel shown in Figure 10. The dynamic time step of integration used is 1.82×10^{-5} s. Figure 13 shows the computed responses and follows the sequence described for Figure 11. Results of the first five natural frequencies are included in Table III.

7.2. Spillway control structure with the embankment fill

7.2.1. 3-D model. Figure 14 shows one panel of the complete spillway control structure with the surrounding embankment soils. The sequence of calculations is the same as for the 3-D model without the embankment fill. Figure 15 is a counterpart of Figure 11 in all its details; geo-materials are not shown in Figure 15(e) for presentation of the mode shapes of the structure. Results of the first five natural frequencies are included in Table III.

7.2.2. Equivalent 2-D model. Figures 16 and 17 are counterparts of Figures 14 and 15; the sequence of calculations is the same as described before; geo-materials are not shown in Figure

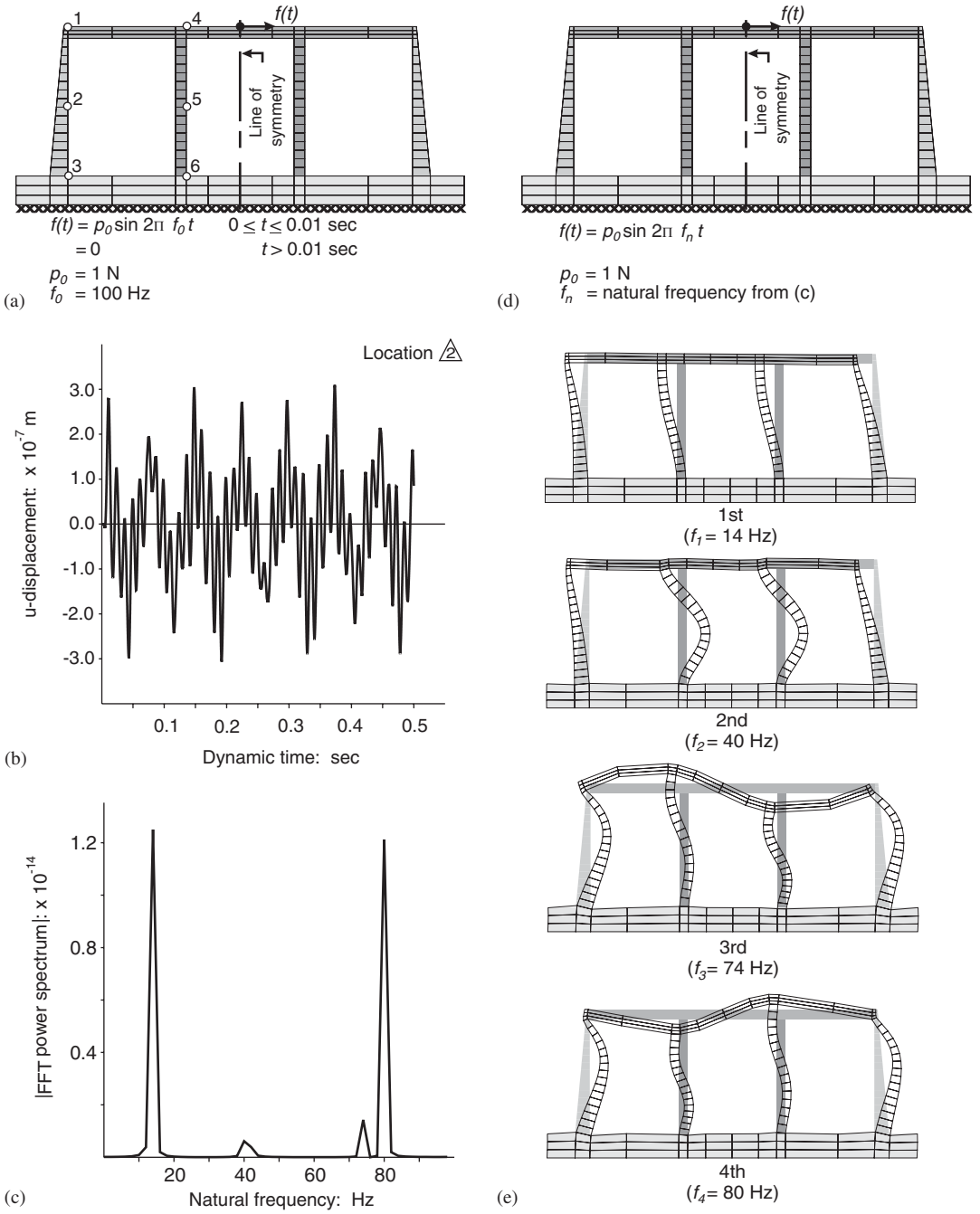

Figure 13. Natural vibrations characteristics of sample problem using the equivalent 2-D model (Figure 12): (a) problem setup for natural frequencies determination; (b) transverse vibrations; (c) natural frequencies via FFT power spectrum of (b); (d) problem setup for mode shape determination; and (e) natural mode shapes (magnified).

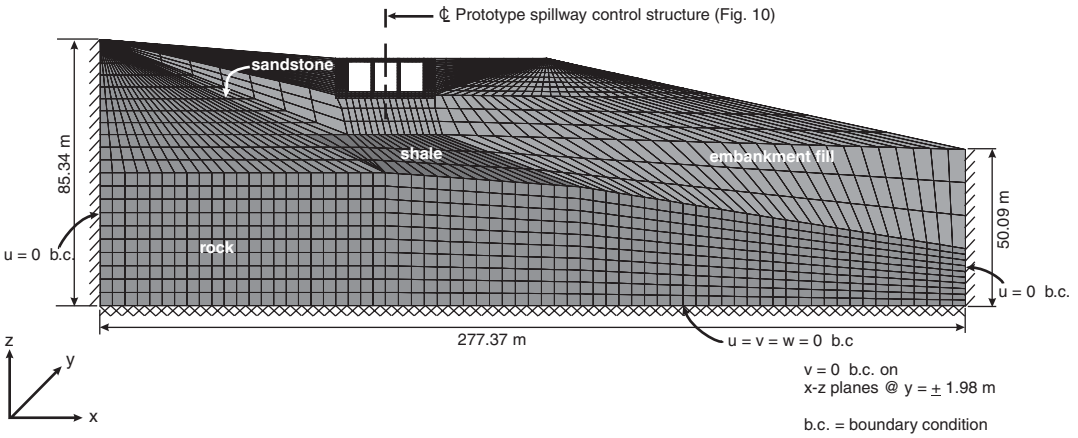

Figure 14. Sample problem—natural vibration characteristics of a spillway control structure with the embankment materials.

17(e) for presentation of the mode shapes of the structure. Again, results of the first five natural frequencies are included in Table III.

Figure 17(f) shows the *w*-displacement versus time history at the same location and in the same analysis for which *u*-displacement versus time history is shown in Figure 17(b). Figure 17(g) shows the FFT power spectrum of the response data shown in Figure 17(f). Resonance response at 4.0 Hz frequency but not at 8.0 Hz frequency is noted in the FFT plot of the *u*-displacement history, Figure 17(c); however, the opposite is true in the FFT plot of the *w*-displacement history, Figure 17(g). Both 4.0 and 8.0 Hz frequencies are included in Table III.

From the deformed configuration of the control structure, Figure 17(e), $f_2 = 8.0$ Hz appears to be associated with rocking mode of vibration.

7.3. Comparison of results

Table III shows the natural frequency values for the four cases of the sample problem analysed. The following observations are based on these results:

(a) presence of embankment soil significantly reduces all natural frequency values of the spillway control structure;
(b) without the embankment fill, natural frequency values for the equivalent 2-D model are much higher than for the corresponding 3-D model; and
(c) with the embankment fill, natural frequency values for the equivalent 2-D model are similar to the corresponding values for the 3-D model.

8. GENERAL COMMENTS

(a) The commonly used numerical procedure for determining natural vibration characteristics of structures with multiple degrees-of-freedom is to solve a matrix eigenvalue

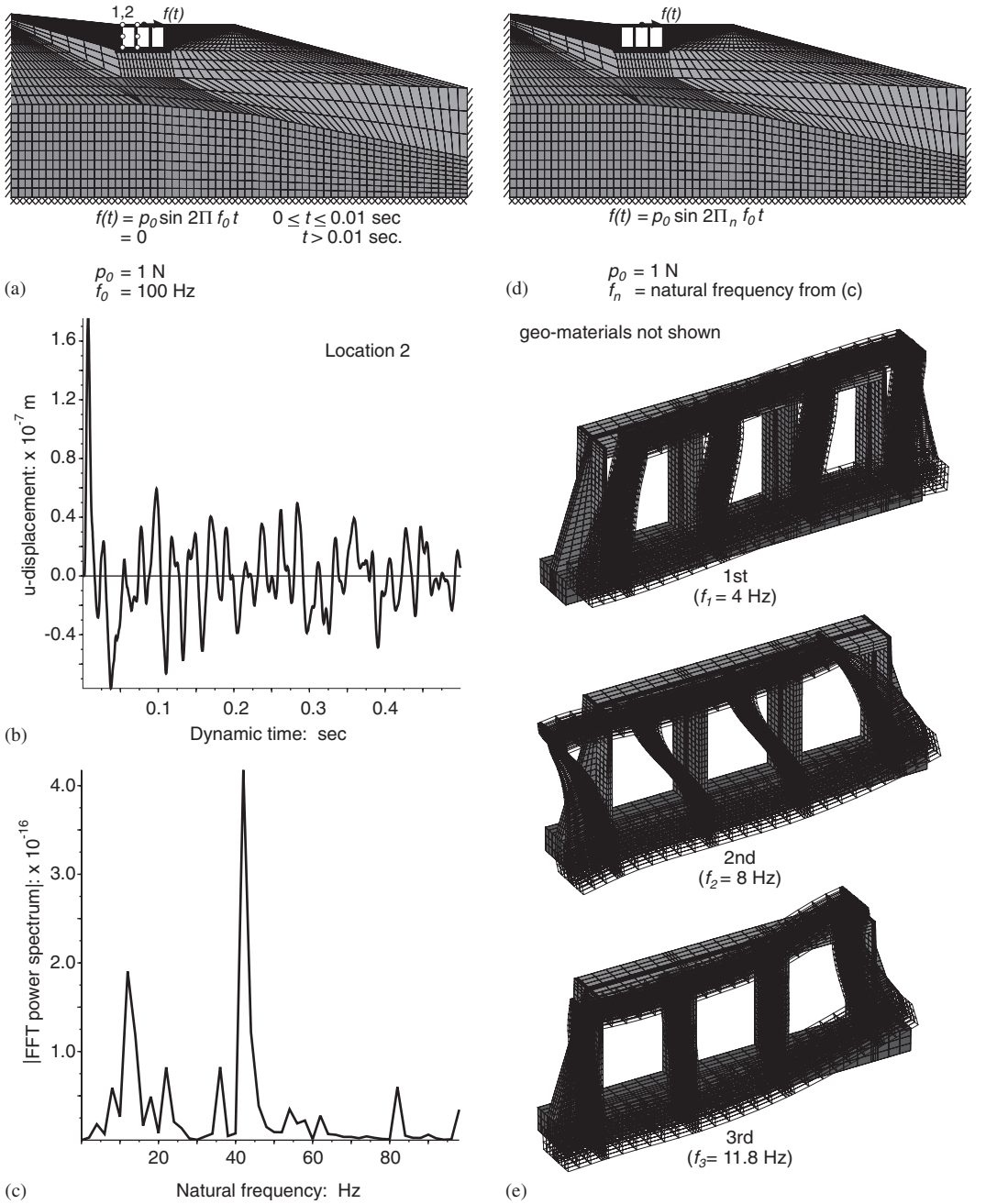

Figure 15. Natural vibrations characteristics of sample problem using the prototype 3-D model (Figure 14): (a) problem setup for natural frequencies determination; (b) transverse vibrations; (c) natural frequencies via FFT power spectrum of (b); (d) problem setup for mode shape determination; and (e) natural mode shapes (magnified).

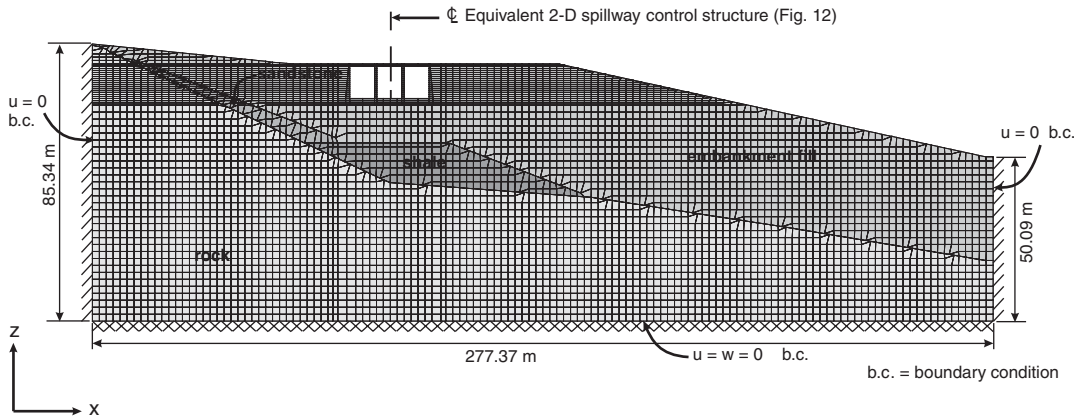

Figure 16. Equivalent 2-D model of sample problem (Figure 14).

problem; other methods used include Rayleigh's, and Ritz's—see References [4, 5, 8] for details. The alternate procedure in Reference [1] follows the rationale of laboratory demonstration in which the free end of a cantilever is pulled in a direction normal to its axis and then suddenly released; the cantilever oscillates back-and-forth, and the record of free vibrations and elapsed time is used to estimate its fundamental frequency. The procedure presented in this paper follows the rationale of field tests to determine dynamic properties of full-scale structures.

(b) The proposed procedure is implemented in a solution scheme which is based on finite difference method—in this method, the continuum is treated as a discretized grid work with all representations of the problem and response parameters lumped at the grid points. However, use of the procedure in a finite element based program has not yet been attempted—in finite element method, the continuum is idealized as an assemblage of elements, and field quantities (stress, displacement) vary throughout each element in a prescribed manner.

(c) The expected features of a structure's response included in Section 4 can be observed in the results of problems included in this paper. Also, the expected response of a structure to a directional disturbance being in all directions, and possible relative ease in identifying natural frequencies from FFT power spectrums of different displacement–time history responses was demonstrated in Figures 9 and 17. With regard to associating a direction of vibration to each of the computed natural frequencies, use of mode shapes was expected to be helpful; this may be more difficult than originally thought, especially in complex structural configurations such as the sample problem in Section 7. For the test problem 3 in Section 6, $f_3 = 5.01\alpha$ appears to be associated with the vertical mode of vibration. For the sample problem in Section 7 (with embankment fill), the $f_2 = 8.0$ Hz appears to be associated with rocking mode of vibration.

(d) It may be desirable to save u-, v-, w-displacement versus time histories at select locations on a structure during the dynamic analysis and to perform FFT power spectrum analyses on all components of the saved responses. In addition to the relative ease in identifying

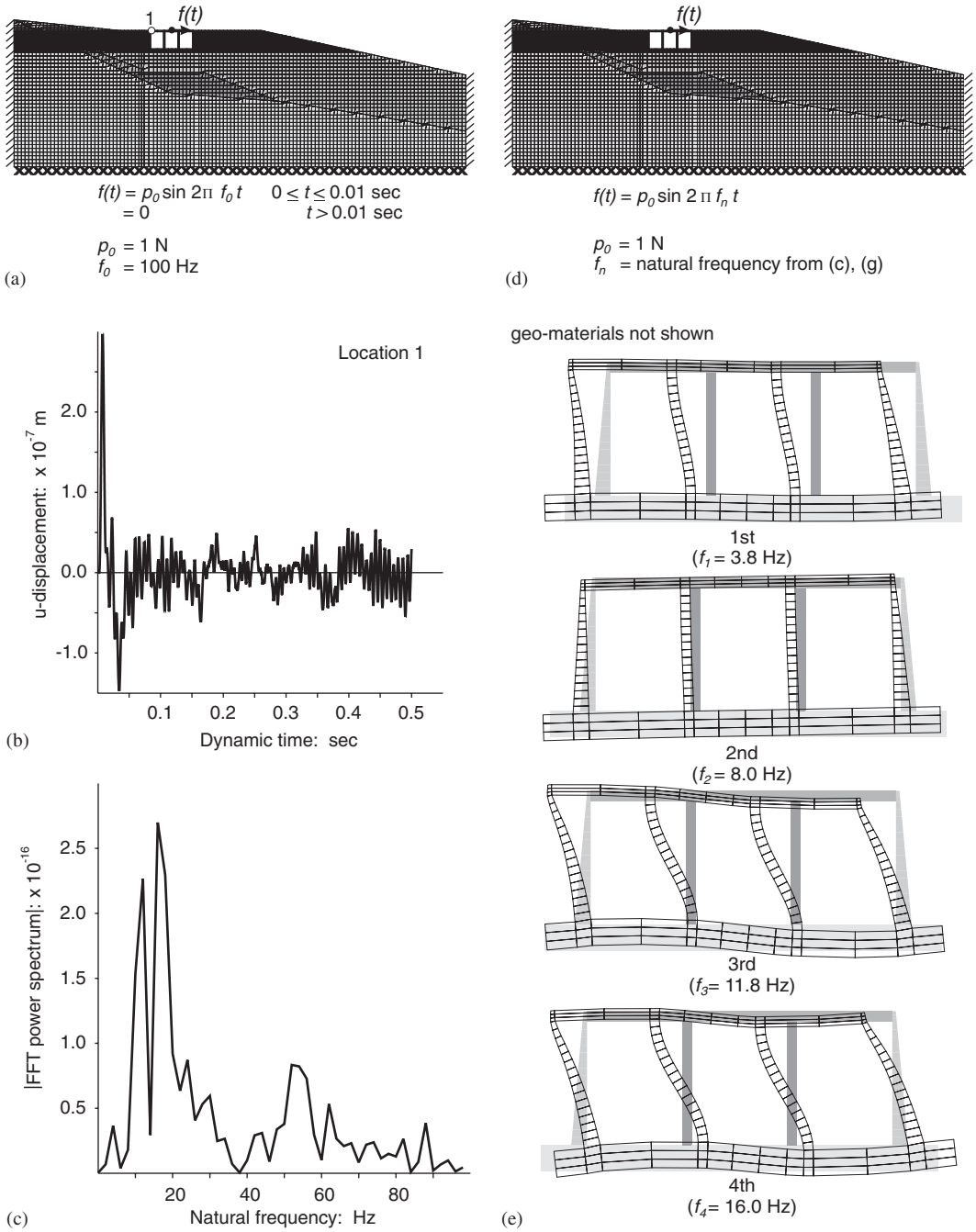

Figure 17. Natural vibrations characteristics of sample problem using the equivalent 2-D model (Figure 16): (a) problem setup for natural frequencies determination; (b) transverse vibrations; (c) natural frequencies via FFT power spectrum of (b); (d) problem setup for mode shape determination; (e) natural mode shapes (magnified); (f) vertical vibrations; and (g) natural frequencies via FFT power spectrum of (f).

Published in 2006 by John Wiley & Sons, Ltd. *Int. J. Numer. Anal. Meth. Geomech.* 2007; **31**:607–648
DOI: 10.1002/nag

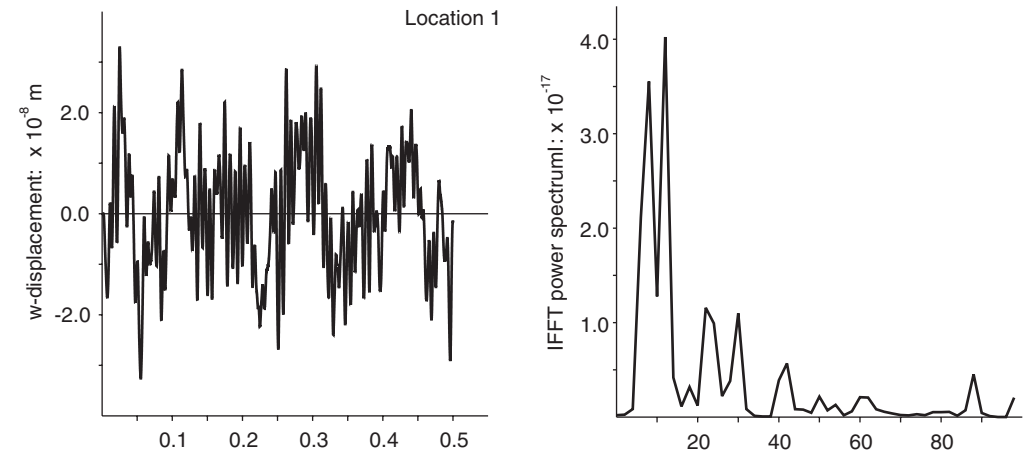

Figure 17. *Continued.*

resonances (natural frequencies) from different directional FFT plots, it may also help identify non-resonating frequency in some of the directional responses; for example, the FFT plots for the *u*- and *w*-displacement—time histories in Figure 17 alternately helped identify the 4.0 and 8.0 Hz natural frequencies.

(e) In numerical analysis, the excitation pulse is evaluated at discrete time steps. Thus, for computational purposes, the frequency spectrum of a sine pulse has a discrete set of frequency values with which the structure is perturbed. Also, the numerical values of the frequencies in the spectrum are in increasing order, Figure 1(b). Thus, a structure responds to each discrete frequency in the order that the discrete frequency gets applied. Therefore, if the excitation pulse is evaluated only at a few time steps, it is likely that the frequencies in the discrete set may be too far spaced to exclude some or all natural frequencies of the structure, and in that case the results from the use of the proposed procedure will not be a complete set of natural frequencies. Thus, for a proper use of the proposed procedure, it is suggested to evaluate the excitation pulse at closely spaced time-steps and to perturb the structure with this large set of frequency values.

(f) The proposed procedure for determining natural vibration characteristics has been used for the kind of problems included in this paper. In principle, the procedure should give useful results for other structural arrangements/configurations and geometries; however, this has not yet been attempted.

(g) All comparisons of mode shape results included in this paper were made by visual inspection only. No attempt was made to compare the locations of inflection points.

(h) It is understood that for usual damping ratios ($\zeta < 0.2$), natural frequencies of structures are not affected significantly by damping; and also that the mode shapes are unaffected by damping. However, damping (if known) can be included in dynamic analysis for natural frequencies using the proposed procedure.

9. MERITS OF THE PROPOSED PROCEDURE

(a) The proposed procedure is for determining all natural frequencies and associated mode shapes of prototype structures via numerical means. In principle, the procedure follows the rationale of forced vibration tests performed on full-scale structures to measure natural vibration characteristics *in situ*; therefore, its use should always give good results.
(b) The proposed procedure uses numerical model's response to the frequencies in the excitation pulse and associates: (i) amplified response to be resonance at or near the natural frequency; and (ii) other response to be regular response to other frequencies. This discrimination of amplified response versus regular response is based on relative (and not absolute) magnitudes of the response amplitudes. It is easy to discern small and large responses in computer-based calculations than it is in field tests where actual responses have to be captured by instruments. In this sense, the proposed procedure is considered robust.
(c) The proposed procedure is computationally efficient. Typically, a well equipped personal computer should be able to complete all calculations for natural frequencies and a few of the mode shapes for a good size model with a grid suitable for dynamic analysis in about eight hours or less. For most problems included in this paper, the time requirements were much less—of the order of five to ten minutes each; the sample problem included in Section 7 took about four hours.
(d) Damping characteristics of a structure/system can only be determined from the response data recorded during a field test. This limitation applies to all numerical and analytical procedures, including the proposed procedure.
(e) The proposed procedure is based on well known ideas and theory; thus, no new learning is required for its use.

10. CONCLUSIONS

(a) The proposed procedure is for calculating all natural frequencies of vibrations and associated mode shapes of gravity structures and yields results that are accurate and compare well with the known analytic solutions and those determined via numerical means/field tests.
(b) The natural vibration characteristics determined from the use of the proposed procedure are complete; that is, no corrections are needed to amend the results as observed in test problem 1.
(c) The proposed procedure is robust and is expected to give useful results for gravity structures as well as other structural arrangements/configurations.

APPENDIX A

The procedure presented in Reference [1] and referred to as an alternate procedure in the paper is based on the premise that the static deflected shape due to the structure's own weight is an appropriate representation of the fundamental mode shape. In this alternate procedure, a problem is solved for static deformation under its own weight by assigning the direction to gravity vector, and then vibratory response is created by setting the gravity vector to zero.

Published in 2006 by John Wiley & Sons, Ltd. *Int. J. Numer. Anal. Meth. Geomech.* 2007; **31**:607–648
DOI: 10.1002/nag

Results for the example problem and test problems 1 and 3 included in this Appendix compare favourably with the first mode of vibration results included in the paper. However, if the static deflected shape due to the structure's own weight is not the fundamental mode shape, then the calculated frequency will not be the lowest natural frequency [4]. Thus, the results of test problem 2 included in this appendix compare well with the second mode of vibration results included in the paper. For the spillway control structure problem, the results included in this appendix are compared with the results of their counterparts using the proposed procedure included in the paper.

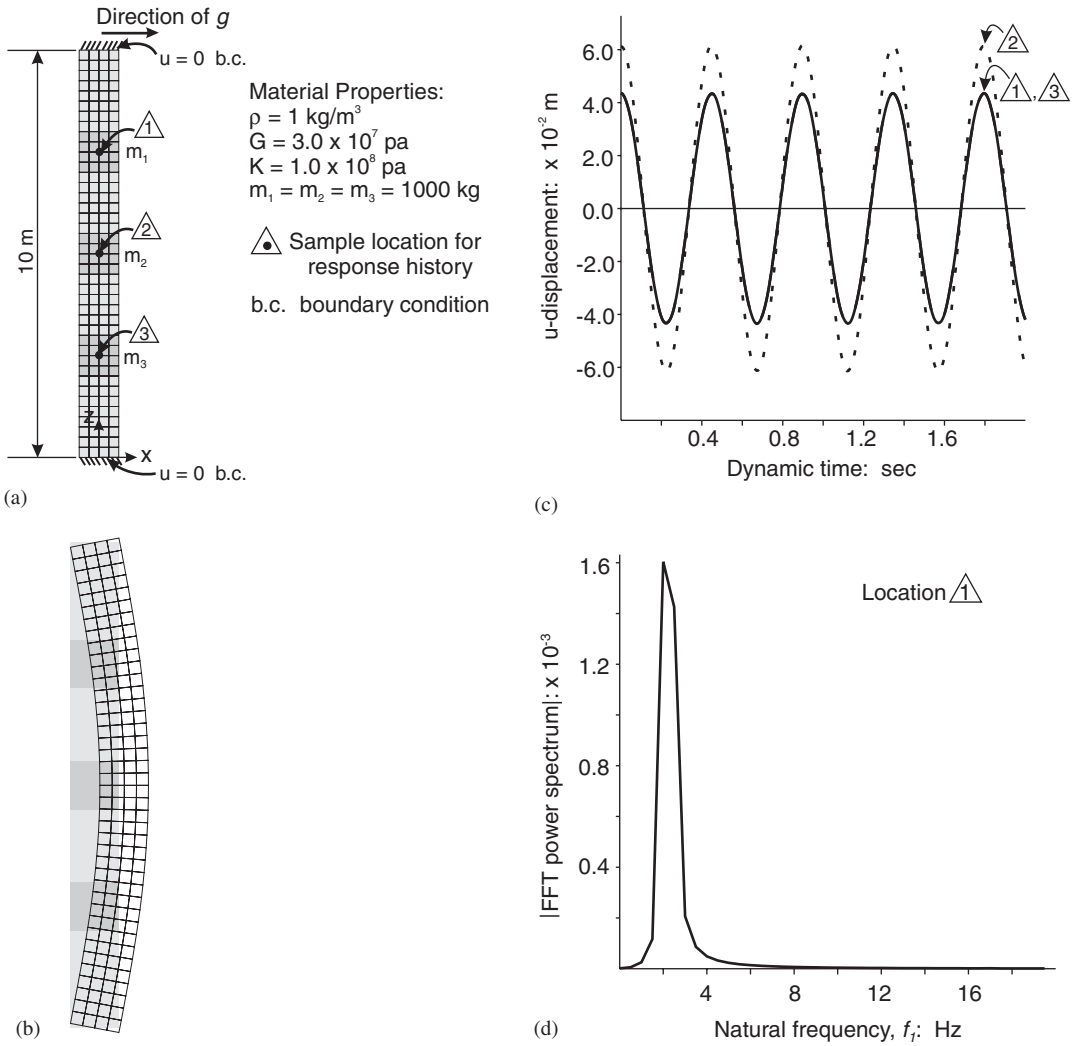

Figure A1. First natural frequency for example problem (Figure 2(b)): (a) problem setup for transverse vibrations; (b) static solution ($g = 10$ m/s^2); (c) transverse vibrations ($g = 0$); and (d) f_1 via FFT power spectrum of (c).

In this appendix, all results are presented in the figures, and only brief comments on each figure are added to conserve space. For each figure, the sequence of presentation is: (a) model setup; (b) static solution under structure's own weight ($g = 9.81\ \mathrm{m/s^2}$); (c) vibratory response ($g = 0$); and (d) an

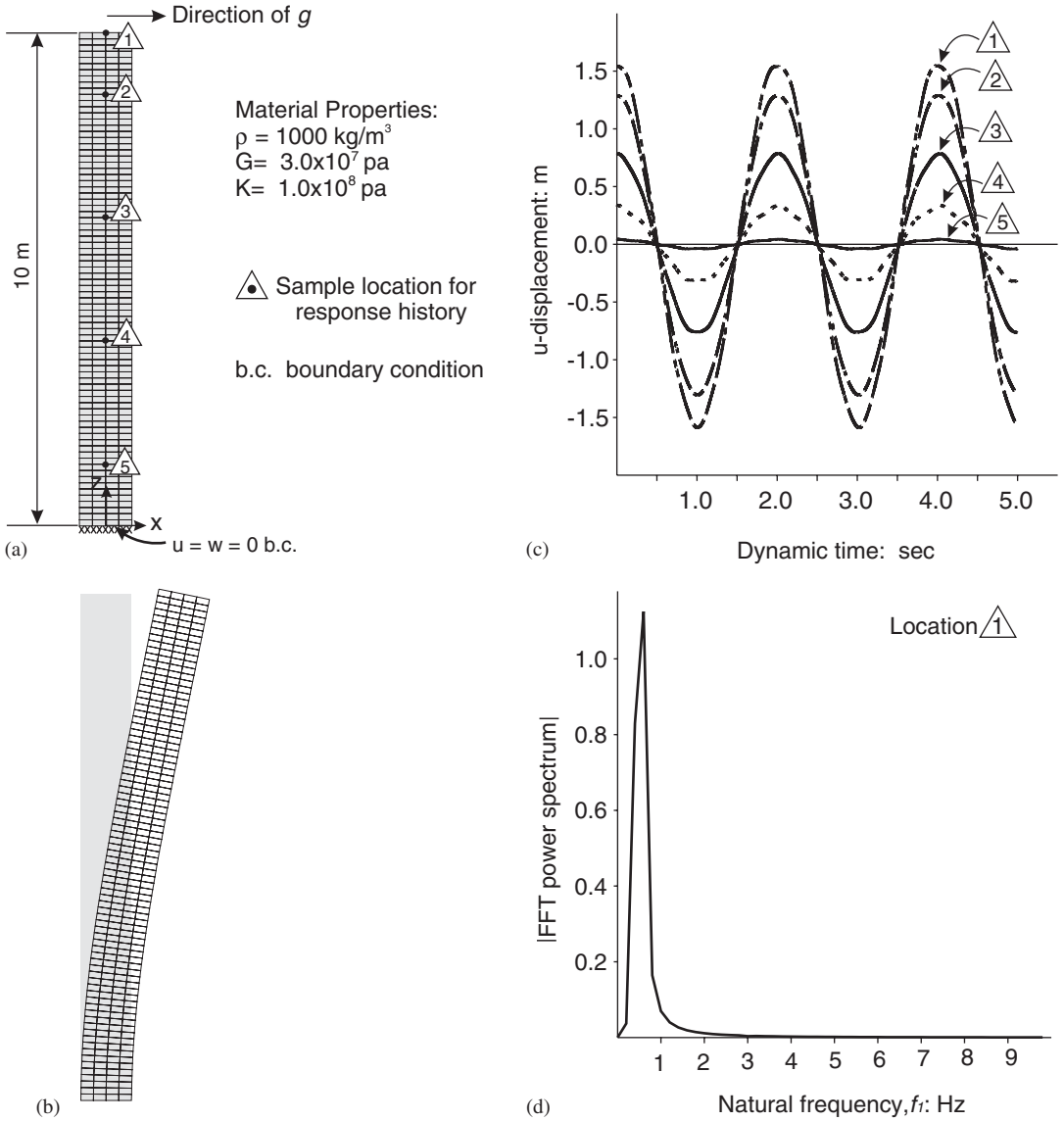

Figure A2. First natural frequency for test problem no. 1 (Figure 4): (a) problem setup for transverse vibrations; (b) static solution ($g = 9.81\ \mathrm{m/s^2}$); (c) transverse vibrations ($g = 0$); and (d) f_1 via FFT power spectrum of (c).

FFT power spectrum of the response data in (c). The static solution plots show the deformed configuration of the structure. As an alternative to the FFT power spectrum, natural frequency can be estimated from the vibratory response plot (number of oscillation cycles divided by the time taken).

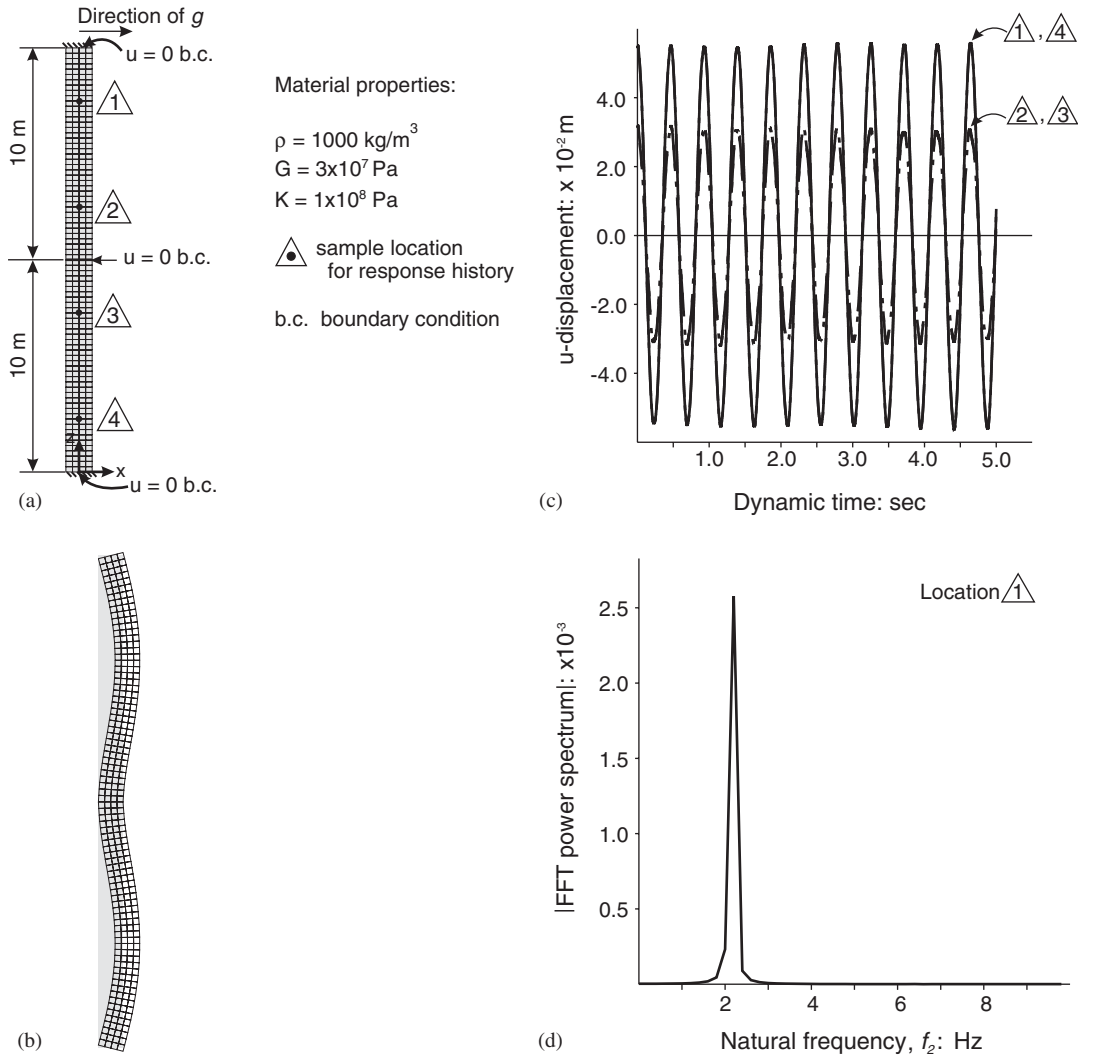

Figure A3. Second natural frequency for test problem no. 2 (Figure 6): (a) problem setup for transverse vibrations; (b) static solution ($g = 9.81$ m/s^2); (c) transverse vibrations ($g = 0$); and (d) f_2 via FFT power spectrum of (c).

Published in 2006 by John Wiley & Sons, Ltd. *Int. J. Numer. Anal. Meth. Geomech.* 2007; **31**:607–648
DOI: 10.1002/nag

(a) Figure A1 shows the alternate solution details for the 1st natural frequency of the example problem shown in Figure 2(b). The computed value of $f_1 = 2.0$ Hz; the corresponding value from Figure 2(f) is 2.04 Hz; and the analytic solution is 2.05 Hz.
(b) Figure A2 shows the alternate solution details for the 1st natural frequency of the test problem shown in Figure 4. The computed value of $f_1 = 0.55$ Hz; the corresponding value from Figure 5(c) is 0.56 Hz; and the analytic solution is 0.46 Hz.

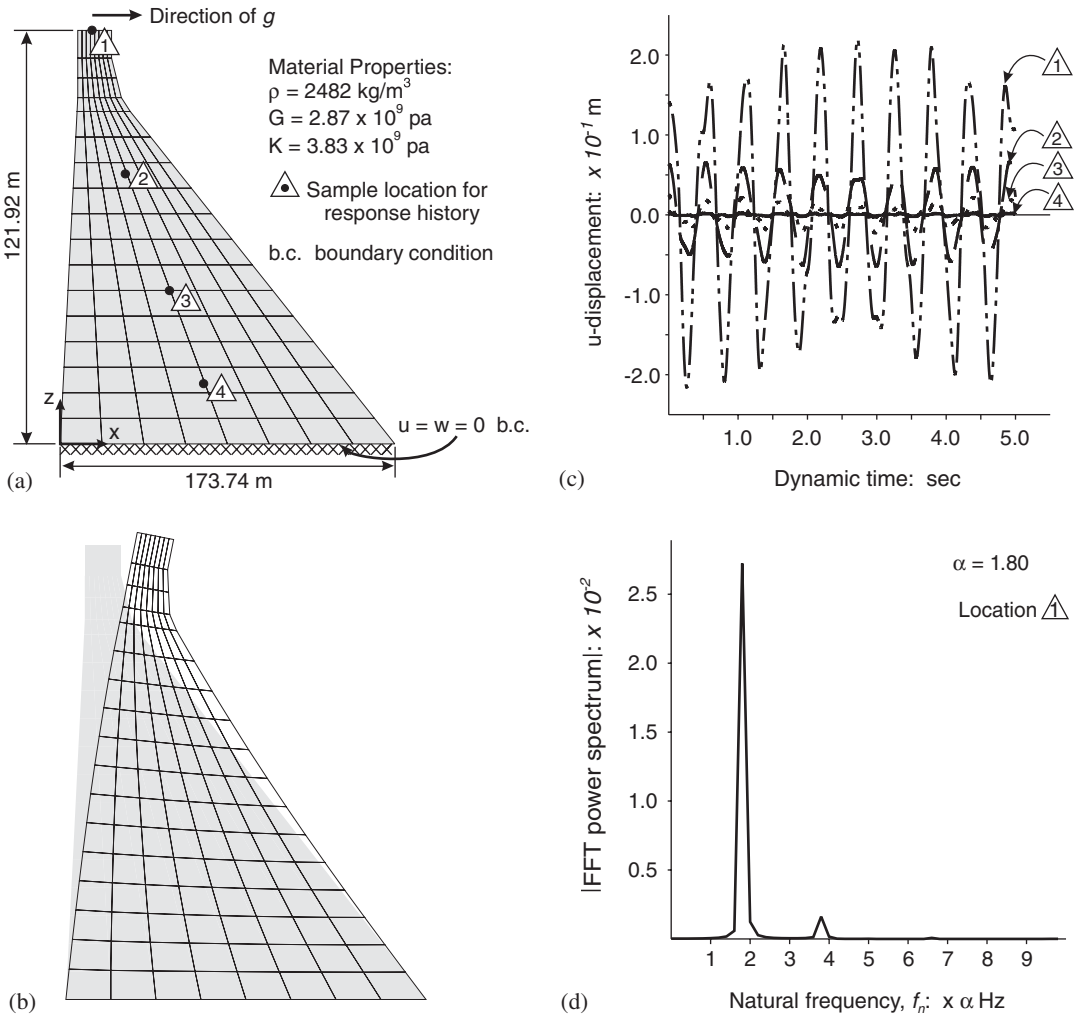

Figure A4. First natural frequency for test problem no. 3 (Figure 8): (a) problem setup for transverse vibrations; (b) static solution ($g = 9.81$ m/s^2); (c) transverse vibrations ($g = 0$); and (d) f_1 via FFT power spectrum of (c).

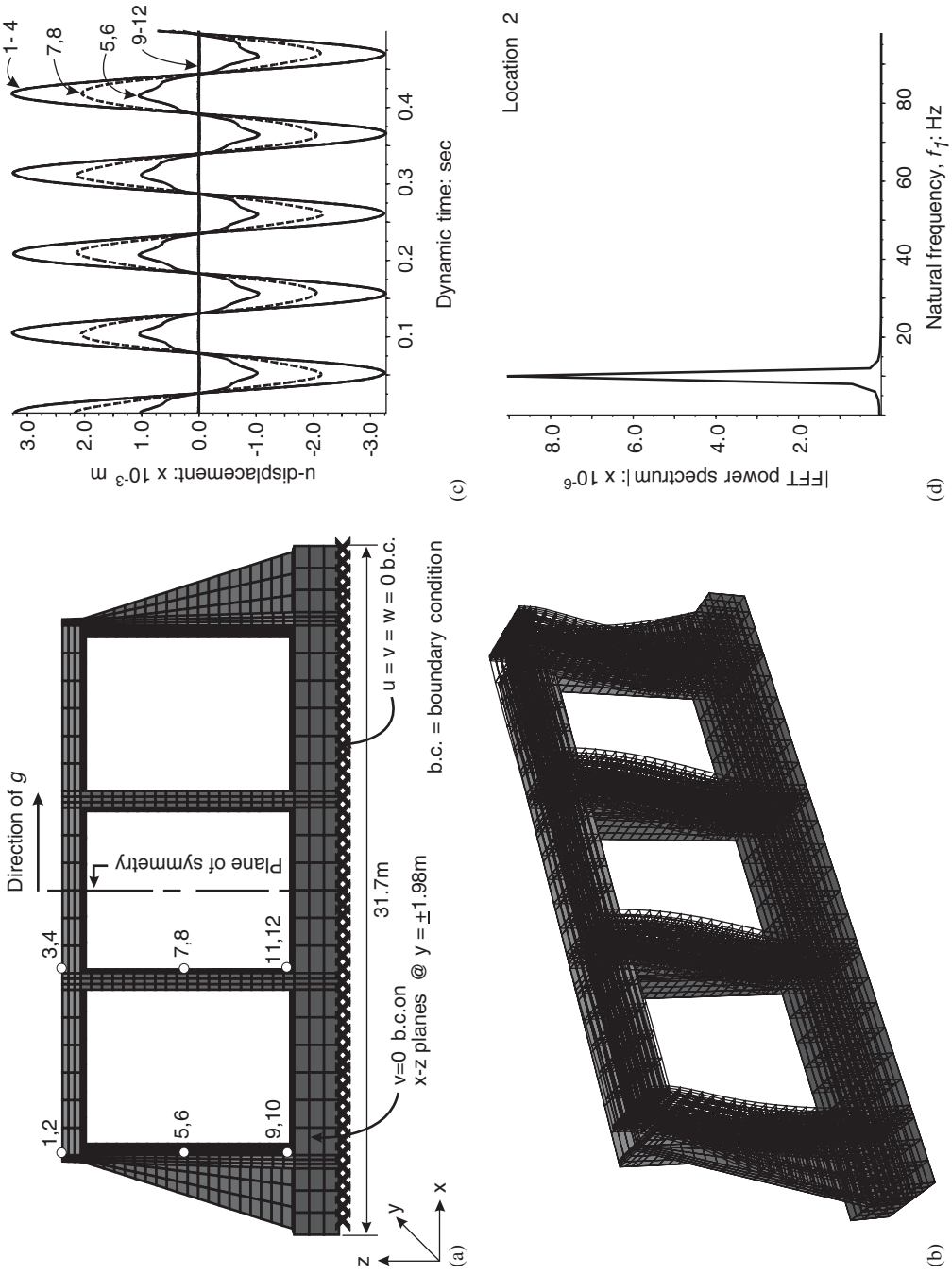

Figure A5. First natural frequency for sample problem using the prototype 3-D model (Figure 10): (a) problem setup for transverse vibrations; (b) static solution ($g = 9.81$ m/s^2); (c) transverse vibrations ($g = 0$); and (d) f_1 via FFT power spectrum of (c).

(c) Figure A3 shows the alternate solution details for the 2nd natural frequency of the test problem shown in Figure 6. Because the deflected shape of the beam under its own weight corresponds to the second mode shape, the computed natural frequency is for the second mode of vibration. The computed value of $f_2 = 2.19$ Hz; the corresponding value from Figure 7(c) is 2.19 Hz; and the analytic solution is 2.02 Hz.

(d) Figure A4 shows the alternate solution details for the 1st natural frequency of the test problem shown in Figure 8. The computed value of $f_1 = 3.17$ Hz; the corresponding value from Figure 9(c) is 3.24 Hz. The 1st frequency values from Reference [10] are: field test, 3.47 Hz with reservoir water; 3-D FEM, 3.70 Hz without reservoir water; and 2-D FEM, 3.14 Hz without reservoir water.

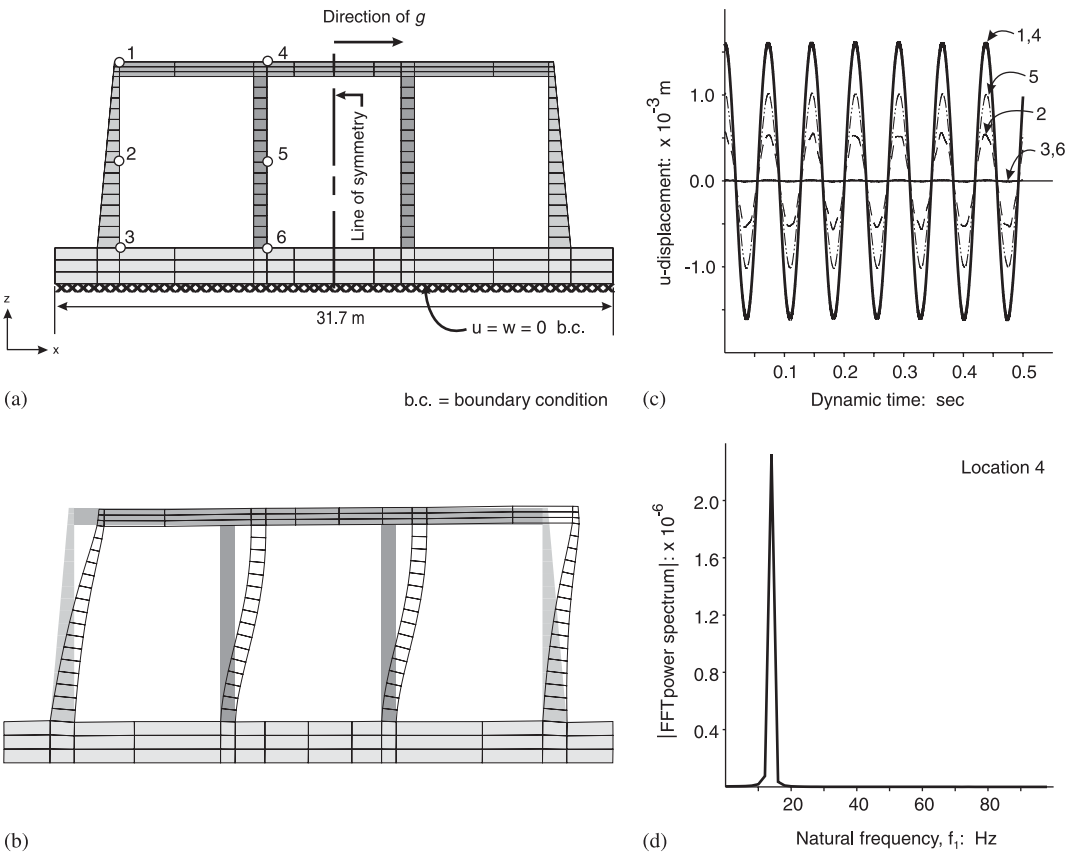

Figure A6. First natural frequency for sample problem using the equivalent 2-D model (Figure 12): (a) problem setup for transverse vibrations; (b) static solution ($g = 9.81$ m/s^2) (c) transverse vibrations ($g = 0$); and (d) f_1 via FFT power spectrum of (c).

(e) Figure A5 shows the alternate solution details for the 1st natural frequency of the sample problem shown in Figure 10. The computed value of $f_1 = 9.57$ Hz; the corresponding value from Figure 11(c) is 10.0 Hz.
(f) Figure A6 shows the alternate solution details for the 1st natural frequency of the sample problem shown in Figure 12. The computed value of $f_1 = 13.8$ Hz; the corresponding value from Figure 13(c) is 14.0 Hz.
(g) Figure A7 shows the alternate solution details for the 1st natural frequency of the sample problem shown in Figure 14. Geo-materials are not shown in Figure A7(b) for presentation of the deformed shape of the structure at the end of the static solution of the problem. The computed value of $f_1 = 3.20$ Hz; the corresponding value from Figure 15(c) is 4.0 Hz.
(h) Figure A8 shows the alternate solution details for the 1st natural frequency of the sample problem shown in Figure 16. Geo-materials are not shown in Figure A8(b) for presentation of the deformed shape of the structure at the end of the static solution of the problem. The computed value of $f_1 = 2.46$ Hz; the corresponding value from Figure 17(c) is 3.8 Hz.

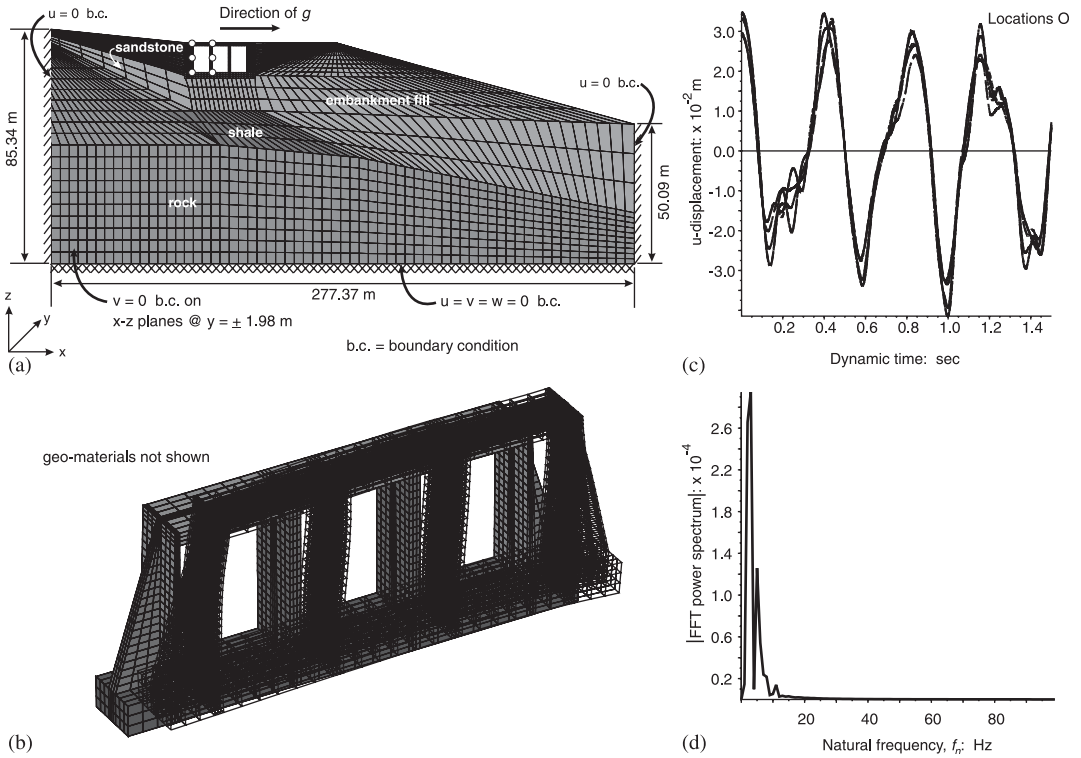

Figure A7. First natural frequency for sample problem with the embankment materials using the prototype 3-D model (Figure 14): (a) problem setup for transverse vibrations; (b) static solution ($g = 9.81$ m/s^2); (c) transverse vibrations ($g = 0$); and (d) f_n via FFT power spectrum of (c).

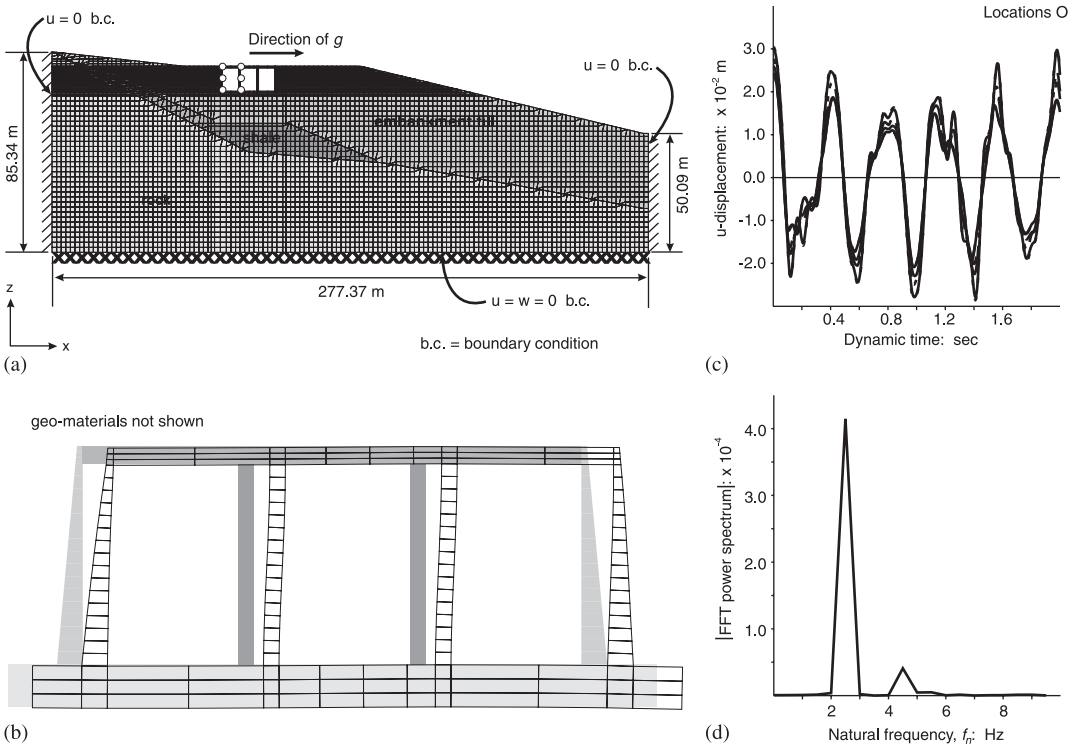

Figure A8. First natural frequency for sample problem with the embankment materials using the equivalent 2-D model (Figure 16): (a) problem setup for transverse vibrations; (b) static solution ($g = 9.81$ m/s^2); (c) transverse vibrations ($g = 0$); and (d) f_n via FFT power spectrum of (c).

ACKNOWLEDGEMENTS

The author would like to express his sincere thanks to Professors Peter A. Cundall and Paul A. Martin for their interest and helpful communications on the subject matter of this paper.

REFERENCES

1. Chugh AK. A counterfort versus a cantilever retaining wall—a seismic equivalence. *International Journal for Numerical and Analytical Methods in Geomechanics* 2005; **29**:897–917.
2. Itasca Consulting Group. *FLAC—Fast Lagrangian Analysis of Continua*. Itasca Consulting Group: Minneapolis, MN, 2000.
3. Itasca Consulting Group. *FLAC3D—Fast Lagrangian Analysis of Continua in 3 Dimensions*. Itasca Consulting Group: Minneapolis, MN, 2002.
4. Chopra AK. *Dynamics of Structures*. Prentice-Hall: Englewood Cliffs, NJ, 2001.
5. Harris CM (ed.). *Shock and Vibration Handbook*. McGraw-Hill: New York, 1988.
6. Pipes LA. *Applied Mathematics for Engineers and Physicists*. McGraw-Hill: New York, 1958.
7. Jacobsen LS, Ayre RS. *Engineering Vibrations*. McGraw-Hill: New York, 1958.
8. Timoshenko S, Young DH, Weaver Jr W. *Vibration Problems in Engineering*. Wiley: New York, 1974.
9. Sutherland JG, Goodman LE. *Vibrations of Prismatic Bars Including Rotary Inertia and Shear Corrections*. Department of Civil Engineering, University of Illinois, Urbana, IL, 1951.
10. Rea D, Liaw CY, Chopra AK. *Dynamic Properties of Pine Flat Dam*. National Technical Information Service: Springfield, VA, 1972.